Synthesis and characterization of Perovskite type nanomaterials and their Novel applications

DISSERTATION SUBMITTED FOR THE AWARD OF THE DEGREE OF

Master of Philosophy
in
Physics

by
Banani Kar
(Enrolment No.- 484/16)

Under the supervision
of
Dr. Anil Kumar Yadav

Department of Physics
School of Physical & Decision Sciences
Babasaheb Bhimrao Ambedkar University
(A Central University)
Lucknow – 226025, U.P., India
2020

DEDICATED

TO

MY PARENTS

AND

MY TEACHERS

DECLARATION

I declare that the dissertation entitled ***"Synthesis and characterization of Perovskite type nanomaterials and their Novel applications"*** has been prepared by me under the supervision of **Dr. Anil Kumar Yadav,** Assistant Professor, Department of Physics, School of Physical & Decision Sciences, Babasaheb Bhimrao Ambedkar University, Lucknow. No part of this dissertation has formed the basis for the award of any degree, diploma or fellowship previously. Further, I declare that the material embodied in the present work is based on original research work and the indebtedness to others has been duly acknowledged at relevant places. This is also declared that the dissertation is essentially free from any kinds of plagiarism.

Banani Kar . 8/9/2020

Banani Kar

Department of Physics
School of Physical & Decision Sciences
Babasaheb Bhimrao Ambedkar University
Vidya Vihar, Raebareli Road
Lucknow-226025,
U.P., India

Date:
Place: Lucknow

CERTIFICATE

This is to certify that the dissertation titled "***Synthesis and characterization of Perovskite type nanomaterials and their Novel applications***" submitted by **Ms Banani Kar** is an original research work and has not been previously submitted in part or full for the award of any other degree or diploma to this or any other university.

The dissertation submitted to Babasaheb Bhimrao Ambedkar University, Lucknow satisfies all the requirements as stipulated in the *Master of Philosophy (M.Phil.)/Doctor of Philosophy (Ph.D.) regulations amended in 2017* and it is fit for submission and evaluation for the award of Master of Philosophy of the University.

Date: 8/9/2020

Supervisor

Head of the Department

विभागाध्यक्ष
Head
भौतिकी विभाग
Deptt. of Physics
बाबा साहेब भीमराव अम्बेडकर विश्वविद्यालय
Baba Saheb Bhimrao Ambedkar University
लखनऊ - 226025 उ० प्र०, भारत
Lucknow - 226025, U.P., India

ACKNOWLEDGEMENTS

It is very pleasure for me to avail the opportunity to convey my heartfelt thanks to **Prof. Bal Chandra Yadav**, Head, Department of Physics, Babasaheb Bhimrao Ambedkar University Lucknow for his invaluable suggestion and constant encouragement.

I consider it my greatest privilege to have worked under the guidance of **Dr. Anil Kumar Yadav**. I hereby express my deep sense of gratitude and indebtness to him for his scholastic guidance, ceaseless encouragement, innovative ideas, suggestions, critical evaluations, incessant devotion of time at every stages of the entire course of my study and preparing this manuscript.

I deem it a unique opportunity and utmost pride to express my profound sense of gratitude to other faculty members **Prof. Devesh Kumar, Dr. Ramesh Chandra, Dr. Khem Bahadur Thapa, Dr. Devendra Singh, Dr. Ravi Kant Tripathi** for their constant encouragement, valuable suggestions, erudite counselling and kind help during the entire period of my work.

I express my sincere gratitude towards **Dr. Surya Gautam, Mr. Diptarka Roy & Mr. Utkarsh Kumar** for providing necessary guidance, constant advice, supervision, suggestions and encouragements strengthened me for executing the research work.

I am indebted to another guide **Ms Priyanka Chaudhary, Mr. Anwesh Pandey, Mr. Sachin Kumar Yadav** without whose advice and supervision it was just impossible to complete the experiment. Their constant guidance, suggestions and encouragements strengthened me for executing the research work.

It was the love, blessings, and encouragements of my Parents **Mr. Biman Kar** and **Mrs. Bijali Kar**, my brother **Mr. Biswadip Kar**, friends and relatives which made it possible for me to complete this work and pursue my educational carrier.

It was his consistent support & encouragement, patience, love to my life, dear **Prasanta** thanks a lot for cherishing my life.

I would like to thank to all my seniors and to my nearest and dearest friends for their consistent support.

I would also thank the **God** Almighty, for His blessings without which I wouldn't have been successful in life.

Banani Kar.

Date: August, 2020

Place: LUCKNOW

(BANANI KAR)

M.Phil. Student

III | P a g e

ABSTRACT

Nanoscience contend with the novel phenomenon of producing, measuring the various properties and to controlling the dimension of an object up of nanometer scale range. Nanotechnology deals with using nanomaterials to develop products for practical application. Perovskite has a remarkable distinct appearance than spinel, due to the single structure. It is able to illustrate extraordinary operations along with an incredibly wide range of phase. Sol-gel technique offers enhanced control over homogeneity, elemental composition and powder morphology. As well, uniformly nano-sized metal clusters can be achieved, which are crucial for enhancing the properties of the nanoparticles. These advantages make the sol-gel route a favourable alternative to other conventional methods for the preparation of ceramic oxide composites. The aim of this work is to develop novel multifunctional nanoparticles. For this purpose, barium titanate nanoparticles were synthesized by the sol-gel process using acetic acid (CA) and PEG as chelating agents, and the effect of chelating agents on surface morphology, size distribution of the synthesized barium titanate nanoparticles have been investigated. The results obtained in this study suggested that pure perovskite barium titanate nanoparticles were obtained with new structural form. Barium titanate nanoparticles formed perovskite structure with a crystallite size in the range of 15.71 nm. This research includes various characteristics of synthesized nanoparticles using various characterization techniques. The present research also deals with the influence on sensing properties. As CO_2 is a colourless and odourless gas, present in environmental atmosphere, it is very hard to identify the increasing concentration, resulting in high damage of mankind moreover of livingbeings. So barium titanate sensor was constructed and used for CO_2 sensing perpuse. We have seen that the sensor also gives response at low concentration of CO_2 gas.

PREFACE

This dissertation, entitled **"*Synthesis and characterization of Perovskite type nanomaterials and their Novel applications*"** sum up the results obtained on practical research carried out in the Department of Physics, Babasaheb Bhimrao Ambedkar University in between 2018-2020 under the supervision of Dr. Anil Kumar Yadav, Assistant Professor, Department of Physics, Babasaheb Bhimrao Ambedkar University, Lucknow.

The work carried out in the present M.Phil. dissertation is divided into 4 chapters.

Chapter 1 contains the basic introduction on nanoscience and nanotechnology, briefly discussing about quantum confinement, outline for fabrication of nanomaterials and lighting on perovskite structure. This chapter also contains tables for literature review which accumulate a comparative study on various perovskite structures and their different sensing properties.

Chapter 2 includes various Synthesis methods utilized for fabricating nanomaterials. Among all these types, sol-gel is researcher friendly because of low cost, can be applied by minimum instrument facility and also at room temperature. This chapter also focused on various characterization techniques which helps us to characterize the synthesized material. We can study various characteristics with the help of XRD, SEM, TEM, UV-Vis, and FTIR spectrometer.

Chapter 3 represents the Synthesis of Barium titanate successfully using sol-gel route. The morphology was observed by SEM analysis. The EDX record approves the development of barium titanate consists of Ba, Ti, O in sample. The crystalline characteristic, formation of phase of the barium titanate was confirmed by XRD analysis. The TEM image

showed the unique internal structure. The FTIR spectrum reveals the presence of various functional groups. The optical band-gap was invented by UV-Vis Spectrometer.

After that the synthesized $BaTiO_3$, used as a room temperature CO_2 sensor, was tested. The differences in the resistance of the film with time before and after exposed to different ppm of CO_2 gas in the closed chamber at room temperature has shown. The minimum response and recovery time were found. The sensor response and sensitivity were also observed at different concentration of CO_2 gas.

Chapter 4 gives the general conclusions drawn from the present dissertation and future research works that would be productive in further understanding the role of nano-oxides for low-temperature applications are desirable.

LIST OF FIGURES

LIST OF TABLES

CONTENTS

CHAPTER 1

INTRODUCTION

1.1 Nanoscience and Nanotechnology

Over the past few decades, a new branch of research, broadly referred to as nano science and nanotechnology has stimulated huge attention across the world not only in terms of fundamental research but also includes various domains in terms of applications and still continues to grow mountingly in notable ways. Nanoscience and nanotechnology can be defined in several ways, some of which are often interchangeable and are extensively deliberated in literatures. Nanoscience is mainly concerned with the fundamental understanding of the phenomena, and the study of materials and systems and their properties lying in the nanoscale of 1~100 nm, whereas nanotechnology covers the vast and diverse range of applications of nanoscience and explains the merger of nanoscience with technology. It is a vast and diverse interdisciplinary field that includes the creation and utilization of the materials, structures, devices and systems through manipulation of matter at nanometer scale [1-3].

Nano? The emergence of the word 'Nano' is reported to take place from a Greek-word ‘nanos’. The word nano literally means dwarf or extremely small, and this accounts to a unit 10^{-9} or one billionth in the SI scaling system. Due to gradual and continuous progress in synthesis of materials, controlling their physical and chemical properties at the nanometer scale for desired applications, tools and techniques for their observation and analysis, the word ‘Nano’ has gradually stepped in and has fit itself into today’s context of scientific advancements and

industrialization, and thus contributing significantly towards the development of novel materials with tailored properties [4-5].

The critical aspect of molecular nanoscience is the design and assembly of well-defined molecular architectures, which laid a milestone in the way of possibilities for fundamental research and applications. Primarily, the tools and techniques associated with nanotechnology deals with a wide range of strategies concerning how the atomic and molecular arrangement governs the properties of matter at nano scale dimensions. Nanotechnology is a key player in the development of materials with new and improved properties. These materials cover a wide range of pre-defined properties such as ceramics, polymers, metals and composite materials etc. However, nanoparticles are those materials ranging to nano scales in all the three dimensions but many times they are unstable and get agglomerated; and therefore, it is essential to protect them and to protect their core-shell structure or various capping agents are used for capping the molecules and prevent them to form a mass [4].

Size regime plays an important role in nano science [5]. Some size dependent applications of nanoparticles have been discussed in the literature such as- particle size lower than 5 nm are used for catalytic activities, particle size smaller than 20 nm is used to soft the hard magnetic materials, particles size less than 50 nm are used for changing the refractive index of the material which is useful for optoelectronic applications, particle size lesser than 100 nm can be used for mechanical strengthening of material and super paramagnetic activity [6-8]. When scaled down to the nanometer scale, various characteristics of the material are influenced by the laws of atomic physics, and the material abruptly exhibit very diverse or enhanced properties as compared to their bulk counterpart. As a result, they possess very unique quality for a bunch of applications. For example, the substances which are opaque

become transparent in nano scale range, e.g. copper; similarly, the bulk materials which are inert, start to show catalytic properties at nano dimensions, e.g. aluminum. Some solid materials become liquid at room temperature after the change of their dimensional scale in nano-range, e.g. gold; several insulating materials turn into conductor when they become nanomaterial, e.g. silicon [6-9]. They have the possibilities for varied electronic, industrial and biomedical applications to get the maximum benefit for welfare of world. Over the coming years, nanotechnology will touch the lives of all of us. Like many scientific advances, it will bring uncertainty and potentials risks too. The nanotechnology is an enabling technology. Various potential market areas for Nanotechnology-products are shown in **Figure 1.1**.

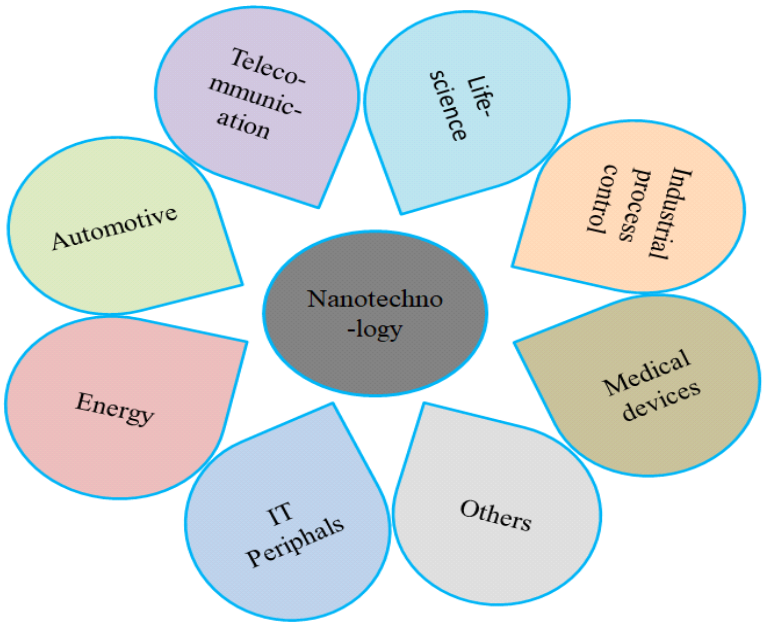

Fig. 1.1: Different potential market areas for Nanotechnology

1.2 The Nanometer Scale

Nanometer scale is used to measure some of the smallest object known to humans. Scientists and engineers are now involved with it to carry out research in some of the most promising frontiers of modern science. A nanometer is fundamentally a unit of measurement in the metric system which is one one-billionth

of a conventional meter (10^{-9} m). To avoid a single atom or a very small group of atoms, the minimum size range of designated nano-objects is usually set to 1nm. So, the nanotechnology deals with the bunch of atoms with at least one one-dimension in nanometer range. The general upper limit is 100 nm, but actually it is a 'free-flowing' limit, which is varying depending on different properties for specific materials. For example, a single strand of human hair measures 100,000 nanometers wide. While a strand of the DNA that tells our body how to make that hair, stands 2.5 nanometers in diameter. So, there are a lot of objects which have dimensions greater than 100 nm, are mentioned as the nanomaterials. Now the query arises that why 1 to 100 nm and not 150 nm? The cause for 1 to 100 nm span is well illustrated because clarification itself concentrates on the outcome of the dimension which holds for a particular material. In Nanoscience, there is not only the small size that is dealing with. There is also the quantum effect, which is size-dependent and significantly different from macroscopic properties of materials. Nanoscience is about the study of materials, which exhibit extraordinary properties, phenomena and functionality because of the impact of small dimensions as compare to bulk. **Figure 1.2** represents the nano-scale consolidation of various nanoparticles and biomolecules.

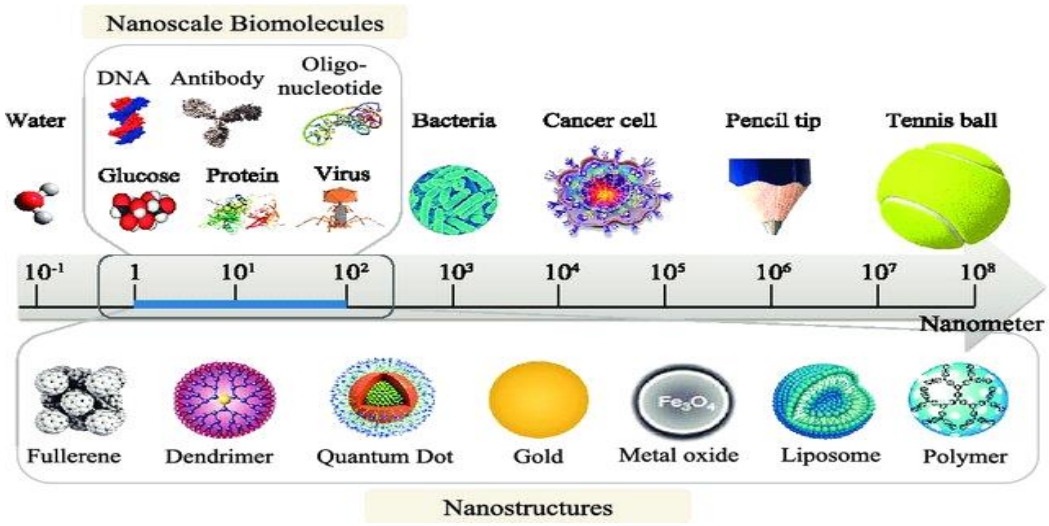

Fig. 1.2: Consolidation of biomolecules and nanoparticles in nano scale [10]

1.3 Quantum Confinement

It is the quantum confinement, which is responsible for enhancement of the difference of energy between the energy state and band gap [11]. This occurrence is directly connected to electronic and optical properties of a particular material. So, when the dimensions of a particle lie in small range, the electronic and the optical properties of that material differ significantly from that of bulk material. When the magnitude of the diameter of a particle is same as the wavelength of electron wave function, quantum confinement effect is observed. For a cubical box with discrete energy levels are given in **Figure 1.3**.

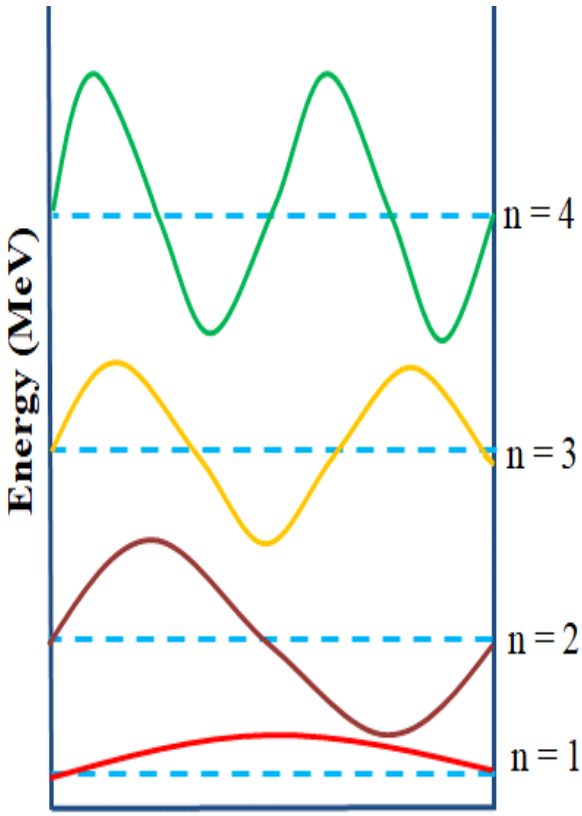

Fig. 1.3: Energy diagram for discrete energy levels

In Nano crystals, electronic energy levels are variable, i.e., similar to bulk materials the levels are not fixed. The energy levels are discrete due to the confinement of electronic wave function to size of the particle. At this stage, Nano

crystal have a drastic change in their optical and electrical properties and thus continuous bands of energy level transforms to the discrete energy levels just analogous to the nature of an electron in a potential well, which is a beautiful phenomenon of quantum mechanics, consequently Nano crystals are allowed as quantum dots too. Furthermore, there is a lofty surface area in nanomaterial which possess very large fraction of atoms on its surface. Since this division depends highly on size, hence it can increase the size effects in physical and chemical properties of the Nano crystals.

Classical mechanics states that if a body possesses enough energy, then it can cross a potential barrier and that energy should be higher than potential energy. If the object has less energy, the probability of finding that particle on another side is null. Whereas according to Quantum Mechanics it is possible that lower energy particle can exist on another side, but the only condition is the energy must be comparable to the size of the wavelength of the particle. It helps to provide a clear picture of nature at subatomic scales in terms of probabilities. Generally, particle's Bohr radius is defined as [12],

$$a_B = \in \frac{m}{m^*} a_0 \quad \text{-------- (1.1)}$$

Where a_0 is denoted for the Bohr radius of hydrogen atom, m stands for rest mass of electron, m* represents the mass of particle and ε is dielectric constant of the material. When the particle size gradually moves towards Bohr exciton radius, due to the quantum confinement effect, excitonic transition energy rises. As a result, a blue shift is happened in luminescence and absorption band gap energy [12]. As for example, when a bulk PbSe shows band gap of 0.28eV, the nano PbSe of diameter 4.8 nm gives an effective band gap of 0.82eV, which exhibit a very strong confined blue shift of >500meV (Bohr exciton radius of PbSe is 46nm) [13]. On the basis of

quantum confinement of different directions, the structures are classified in three different categories like quantum dot, quantum wire and quantum well. The basic variety of quantum confined structures is given in **Table 1.1.**

Table 1.1: Classification of different quantum confined structures with their free dimension

Structure	Quantum Confinement	Free dimensions
Bulk	0	3
Quantum well	1	2
Quantum wire	2	1
Quantum dots	3	0

For quantum dots, there are all the three dimensions in which the charge carriers are confined. As a result, the electrons manifest atomic-like discrete energy spectrum. Quantum wires are formed, when the confinement is in two dimensions. For quantum well, the electrons and holes (i.e. the charge carriers) are restricted to move in plane and they are free to change their position in 2D plane. So, energy levels become discrete which were continuous before quantum confinement. In quantum well, the density of electronic states is higher near the edges of valence and conduction band as compared with bulk material. Therefore, concentration of carriers is high enough for contribution of band edge emission [14]. **Figure 1.4** shows the density of electron states as function of different dimensions.

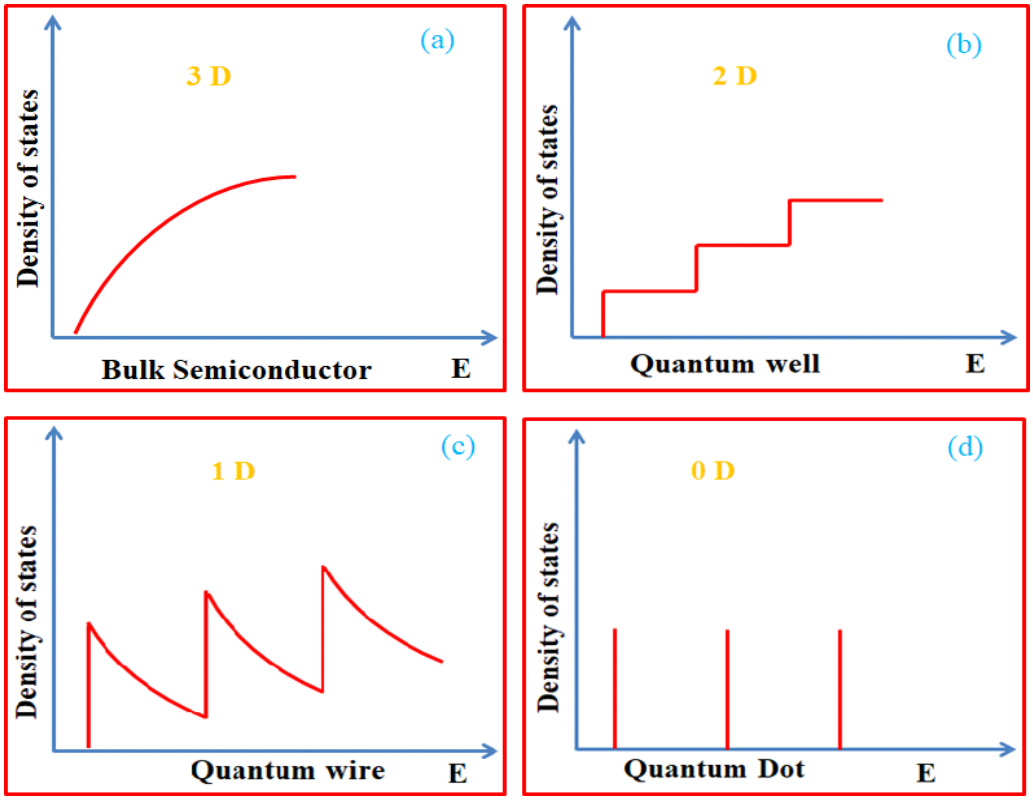

Fig. 1.4: 3D, 2D, 1D and 0D materials along with their density of state curves

1.4 Fabrication of Nanostructured Materials

By controlling the properties of nano-dimensional structures, we are leading towards the new science, moreover towards new technologies, devices, and products. Nowadays, the most feasible industrial scheme to make nanostructures is top-down action-plan. On the basis of photolithography, in addition with the requirement of smaller devices the top-down method also gives challenges to the physical limitations of the miniaturization of microelectronics [14]. In last few decades, because of the arrival of new synthesis method for creating nanoparticles, the Nano science and nanotechnology has been staying on higher rank of explosive growth. With the help of so called "bottom-up" processing, and with the development and noteworthy assistance of electron microscope, the nanotechnology reveals a new art for living beings. The different synthesis methods for synthesis of nanomaterial take a survey in organic, inorganic and biological system to control the structure, shape and size.

There are large numbers of pathway that have been formulated to synthesize different nanomaterial of various dimensions in gaseous or liquid phase. With the development of two synthesis technologies that are "top-down" and "bottom-up", finally there are opening of two convergence approaches of nano-based products for practical purpose, both to interact with outer world and to tailor the nano-scale device. The bottom-up method gives permission to control the structural and chemical architecture; though the manual gathering of exclusive nano-sized components is clearly prohibitory in cost and time. **Figure 1.5** shows the two synthesis approaches for producing nanomaterial.

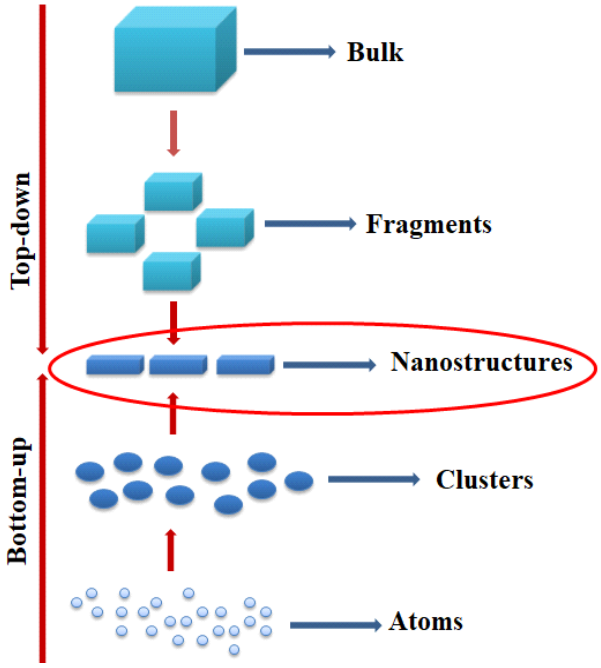

Fig. 1.5: Synthesis approaches for nanomaterials

1.5 Variation in Properties of Nanomaterials

Most of the nanomaterials are crystalline in nature and they possess a unique property. Nanomaterial show unprecedented changes in chemical, physical, mechanical, magnetic, etc., when are reduced from bulk to nano range. Some of the changes are briefly discussed below:

1.5.1 Physical Properties

At the nano-scale, surface area to volume ratio increases. This alters the surface pressure and consequently results in a change in the interatomic spacing. Crystal structure of the nanomaterial is same as bulk material, only the change is observed in lattice parameters [15]. The inter-atomic spacing (d_{hkl}) is also decreased due to long electrostatic force and because of reduction in size. Hence, the melting point in nanomaterials also differs in comparison with their bulk.

1.5.2 Chemical Properties

Due to increase in surface area in comparison with the volume, the catalytic activity can be observed in nanomaterial. Moreover, crystal structure of nanomaterial and size dependency is influenced by the synthesis technique used.

1.5.3 Mechanical Properties

Elastic strain, stress, Young modulus, hardness of the material, etc. and other mechanical properties also varies as the material reduced to nano dimension [16].

1.5.4 Electronic Properties

Electronic structure of the nanomaterial is different from the bulk material and a band gap is created when the difference in energy level is more than KBT. The density of energy state is also changed in the conduction band because of change in electronic arrangement of the nano-ordered material. Ionization potential of nano dimensional materials is higher than the bulk materials of the same composition.

1.5.5 Magnetic/ Dielectric Properties

Nanoparticles made of semiconducting material like silicon, germanium etc., are not semiconductors. Ferrites show extraordinary magnetic and dielectric properties [17]. Their magnetic properties depend on the sintering temperature and sometimes on the dopant concentration.

1.6 Applications of Nanomaterial

Nanotechnology is a boon to the modern world of science and technology. There are plenty of applications of the nanomaterials and most present applications embody evolutionary progresses in existing technologies. Some key applications are discussed in brief as below:

1.6.1 Automotive Industry

Nanomaterials are used as sensors. Palladium nanoparticles are used in hydrogen sensor [18]. They are used for painting and also used as a catalyst. They are used for manufacturing light weight devices.

1.6.2 Electronic Industry

Miniaturization of electronic devices, compact size and less power consumption enhance the use of nanomaterial in the electronic industry. They can be used in FET, MEMs, LED display, Laser diode, coating materials, filters, fibers, etc. [19-20].

1.6.3 Chemical Industry

Nanomaterials are used as fillers in chemical industries. They are used for preparing dyes, ceramics, plastics, etc. [21]. Nano composites are used for the coating material.

1.6.4 Medical Field

Polymeric micelle nanoparticles are used in drug delivery. Iron nanoparticles are used for breaking clusters of bacteria in chronic bacterial infection, whereas silver nanoparticles are used in the treatment of cancer etc. [22]. Nano diamond- the nanoparticles of carbon is used in joint implantation. Ceramic oxide nanoparticles used as an antioxidant for removing oxygen free particle from blood which helps in reducing traumatic injury. They are also used in chemotherapy [23].

1.6.5 Energy Sources

Nanoparticles of the semiconductor are used in the solar cell [24]. They are also used in designing of solar panels, solar devices, etc. Furthermore, the nanoparticles are used for creating electrodes in the fuel cell.

1.6.6 Food

Nanotechnology is also used in the food industry from growing of foods to its packaging. Nano materials are developed for the change of flavors as well as hygienic food to eat it [25].

1.6.7 Cosmetic

Nanoparticles are used in many sunscreen lotions/creams. They are used in various gel, soap, hand wash, etc. They are also used in toothpaste.

1.7 Perovskite

Ceramics are the largest and most widely used materials by mankind. It is very rare to find particular ceramic phases naturally in the earth which may be used profoundly by human society for various technological aspects [26]. Among the multifunctional ternary structures, usually, the phases which are recognized by A_2BX_4 and ABX_3, represent the spinel and perovskite structures, respectively. Perovskite has a remarkable distinct appearance than spinel, and due to the single structure along with the proficient chemical manipulation are able to illustrate completely different operations along with an incredibly wide range of phase [26]. The name Perovskite has been derived from a structural family of a particular mineral with the composition similar to $CaTiO_3$. Perovskite-type oxides are the materials that follow the structure ABO_3 where A and B represent the alkaline earth metal and transition metal, respectively as shown in **Figure 1.6**. The cations with larger and smaller ionic radius hold the position A and B of that very structure, respectively [27]. The contradiction

between structural and compositional properties is often seen in the field of material science, which is seldom possible to explain clearly [26]. The photo catalytic activity of the material depends on several factors such as the effective mass of electron and hole, exciton lifetime, exciton binding energy, diffusion length, etc. Those factors influence the charge separation and transport process inside the crystal lattice [28].

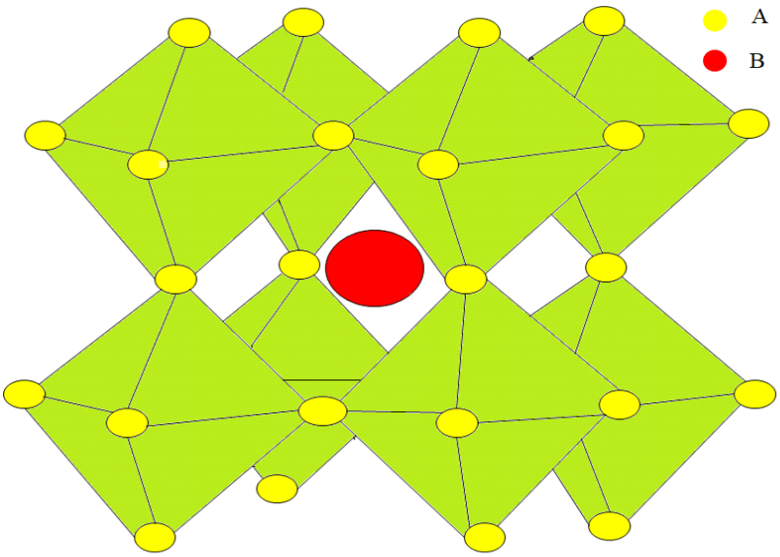

Fig. 1.6: Structure of perovskite

Jocker and Van Saten studied for the first time the magnetic properties of the perovskite structure. They are the class of ferrites with rare earth metal and are canted antiferromagnets. The structural formula of ortho-ferrite is ABO_3 where A represents rare earth metal ion. Small trivalent and tetravalent atoms occupy the center position of the cube and large divalent and trivalent molecules occupy the corner position of the cube. In the orthorhombic structure, the four octahedral in the unit cell are tilted in different directions, the extent of tilting being measured by non-linearity of B-O-B bond angles. The ABO_3 perovskite exhibits different electronic and magnetic properties at different temperature depending on 3d electronic configurations of the

transition metals. In octahedral coordination, cations with configurations 3dN (where N = 4, 5, 6 or 7, corresponding to Mn(III), Fe(III), Co(III) and Ni(III), respectively), may exist in either a spin-paired ground state or in states with maximum unpaired electrons according to Hund's rule.

1.8 Sensor

A sensor is a device that produces a measurable output as a function of input given. They are useful in-situ measurements such as in industrial process, scientific applications, daily necessity, offices, etc. They act as critical components in all measurement and controlled applications, responsible for converting any physical phenomenon such that temperature, pressure etc. into a measurable quantity through data acquisition (DAQ) system. It does not perform itself; it acts as a part of larger assembled system that may incorporate many other devices such as a transducer, detectors, data recorders, signal conditioners, signal processors, memory devices, actuators, etc. Sensors can be classified into three types:

1.8.1 Physical Sensors

A physical sensor is based on the measurement factor where no chemical reaction occurs. Measurement can be in the form of absorbance, temperature, mass, refractive index, conductivity, etc. Temperature sensor, Pressure sensor etc. are well known physical sensor [29-31].

1.8.2 Chemical Sensors

A chemical sensor is a sensor in which analyst participate to perform a chemical reaction and to give an analytic signal corresponding to the input. Various gas sensors and humidity sensors are well known chemical sensor [32-33].

1.8.3 Biosensor

Sensor that is used in biological applications is termed as biosensors. Immuno sensor, Microbial potentiometric sensor, etc. are the example of biosensors [34-35].

1.9 Materials and Literature Review

Nowadays perovskite is in the center of research interest in the field of sensing technology. Perovskite sensor can be operated at very low temperature and it gives better sensitivity and sensor response than the other metal oxides. Literature survey related to $BaTiO_3$, $LaFeO_3$, $Bi_{0.5}Na_{0.5}TiO_3$, their synthesis, characterizations with different sensing parameters is depicted in **Table 1.2** & **1.3.**

1.9.1 International Status

Table 1.2: Literature survey on various type of nanomaterial and their various sensing applications at the International level.

S. No.	Material	Synthesis Method	Chemical used	Crystallite Size or Thickness /porosity	Properties or application of the content	Ref.
1.	$BaTiO_3$	Solid state reaction/spin coating	Polyvinyl butyl, 2-2 butoxy ethoxy ethyl alcohol, PEG	200-500nm	Gas sensing properties	[36]
2.	$SrTiO_3$/ $BaTiO_3$	Sol-gel/ spin coating	Titanium butoxide, Barium acetate, strontium acetate, acetic acid	40 nm by XRD	Ethanol Gas Sensor	[37]

3.	$BaTiO_3$ / $BaSbTiO_3$	Balling Method	$BaTiO_3$, Sb_2O_3, graphite powder, ethyl alcohol	100 μm	CO and N_2 Gas sensing	[38]
4.	$BaTiO_3$ /$SrTiO_3$	Solution based synthesis	Barium titanium, Strontium titanate, oleic acid and Isopropoxide	5-60 nm diameter of nanorod	Study of cubic perovskite nanorods	[39]
5.	$BaTiO_3$	Electrochemical method	Barium hydroxide, ethanol	15 nm nanowire	Photoluminescence spectrum of $BaTiO_3$	[40]
6.	$BaTiO_3$	Sol-gel/dip coating	Barium acetate, Glacial acetic acid, tetra ethoxy titanate, ethanol	Very thin film 44 nm	Thermal, optical and dielectric properties	[41]
7.	$BaTiO_3$ - Y_2O_3	Sol-gel	Barium acetate, Y_2O_3,glacial acetic acid	1-2 μm	DTA/TGA measurement, Positive Temperature Coefficient of resistivity(PTC	[42]

8.	$BaTiO_3$	Hydrothermal reaction	Barium Hydroxide, Titanium oxide	50-200 nm	Study of Raman Spectroscopy	[43]
9.	$LaFeO_3$	Simple synthesis route	La nitrates, Fe nitrates, Sorghum straw, citric acid	20-30 nm	Acetone sensing	[44]
10.	$LaFeO_3$	Polyconden-sation of Glucose, hydrothermal method	Glucose, Fe nitrate, La nitrate, carbon sphere, distilled water	50 nm	Formaldehyde sensing	[45]
11.	$LaFeO_3$	Hydrothermal method	Fe nitrate, La nitrate, citric acid	19.2 nm	Acetone gas sensing	[46]
12.	Co-doped $LaFeO_3$	Chemical coprecipitation	Fe nitrate, La nitrate, $Co(CH_3COO)_2.4\ H_2O$, $(NH_4)_2Co_3$	21nm- 28nm	Ethanol gas sensing	[47]
13.	TM (Mn, Co, Cu) doped $LaFeO_3$	Glycine nitrate process, citrate auto combustion process	Fe nitrate, La nitrate, Mn nitrate, Co nitrate, Cu nitrate	20-50 nm	TM doping properties based on visible light	[48]

14.	BNT	Hydrothermal	NaOH, Bi_2O_3, TiO_2	400nm Nano plate & 50-100 nm nanowire	Morphology controlled synthesis and growth mechanism	[49]
15.	BNT	Sol-gel/ spin coating	Bi nitrate, $NaNO_3$, Titanium iso-propoxide	50-200 nm	Thermal analysis	[50]

1.9.2 National Status

Table 1.3: Literature review on different types of nanomaterials and their sensing applications at national level.

S. No.	Material	Method used for synthesis	Chemical used	Crystallite Size or Thickness /porosity	Properties or application of the content	Ref.
1.	$BaTiO_3$	Spray pyrolysis	Barium chloride, Titanium chloride	40 nm by XRD	Gas sensing (LPG) at room temperature, sensitivity 3.03 at 350ºC	[51]
2.	$BaSrTiO_3$	Mechano chemical Process/ Screen printing	Barium hydroxide, titanium dioxide, strontium hydroxide	264 nm by XRD	Ammonia Gas Sensing	[52]
3.	$BaTiO_3$	Sol gel/ spin coating	Barium acetate, glacial acetic acid and butoxide	0.5- 5 μm	I-V Characteristics, CV Characteristics	[53]
4.	$BaTiO_3$	Ball milling	BaO, TiO_2	20-50 nm	Mechanochemical activation by thermal treatment	[54]
5.	$BaTiO_3$	Spin coating	$BaTiO_3$ powder, HNO_3	9.5 nm	Functional group identification by optical characterization	[55]

6.	$BaTiO_3$-$SrFe_{12}O_{19}$	Sol-gel	Barium acetate, n-butaoxide, 2- methoxy ethanol, Sr-nitrate, Fe nitrate	400-600 nm	Effect of constituent, phase variation, ferroelectric, dielectric and magnetic properties	[56]
7.	Sr-doped $LaFeO_3$	Solution combustion method	La nitrates, Fe nitrates, Sr nitrates, diethyl oxalate, formaldehyde	0.067- 0.028 μm	Change in surface area and properties on changing doping %	[57]
8.	Ba doped BNT	Solid state reaction	Bi_2O_3, Na_2CO_3, $BaCO_3$	0.54- 0.56 μm	Dielectric and conductivity properties	[58]
9.	BNT	Ball milling	Na_2CO_3, Bi_2O_3, TiO_2, alcohol medium	100 nm	Phase transition by dielectric and internal friction	[59]
10.	$LaFeO_3$	Auto combustion and modified penchini method	La nitrate, Iron nitrate, citric acid	46 nm	Butane sensor	[60]

References:

1. H.S. Nalwa, Handbook of nanostructured materials and nanotechnology, Academic Press, San Diego, Vol. 1, (2001).
2. N. Taniguchi, On the basic concept of nano-technology, Proc. Int. Conf. Prod., London, Part II, British Society of Precision Engineering (1974).
3. R. Birringer and H. Gleiter, Encyclopedia of materials science and engineering, Suppl. Vol. 1, Pergamon Press, Oxford, U.K., (1988).
4. J. Stohr, H.C. Siegmann, Magnetism: from fundamental to nanoscale dynamics, Springer 146 (2006) 33.
5. W. Kern, K. K. Schuegraf, Handbook of thin film Deposition and Techniques: Principles, Methods, Equipment and Applications (Krishna Seshan, Ed.) Norwich, N.Y. Noyes Publications/ William Andrew Pub. (2002) 11.
6. A.J. Clarkson, D.A. Buckingham, A.J. Rogers, A.G. Blackman and C.R. Clark, Nanostructured ceramics in medical devices: applications and prospects, Journal of the Minerals, Metals and Materials Society 56 (2004) 38-43.
7. M. Boukallel, M. Gauthier, M. Dauge, E. Piat and J.Abadie, Smart micro robots for mechanical cell characterization and cell convoying, IEEE Trans. Biomed. Eng. 54 (2007) 1536-40.
8. Cristina Buzea, Ivan Pacheco and Kevin Robbie, Nanomaterials and nanoparticles: Sources and Toxicity, Biointerphases, 2 (2007) 17-71.
9. R.C. Shetty, Potential pitfalls of nanotechnology in its applications to medicine: immune incompatibility of nanodevices, Med. Hypotheses 65 (2005) 998-999.

10. Saallah, S., & Lenggoro, I. W. Nanoparticles carrying biological molecules: Recent advances and applications. KONA Powder and Particle Journal, 35 (2018) 89-111.

11. Delley, B., and E. F. Steigmeier. Quantum confinement in Si nanocrystals. Physical Review B 47(3) (1993) 1397.

12. Yoffe, A.D. Low-dimensional systems: quantum size effects and electronic properties of semiconductor microcrystallites (zero-dimensional systems) and some quasi-two-dimensional systems. Advances in Physics, *42*(2) (1993) 173-262.

13. Wise, F.W. Lead salt quantum dots: the limit of strong quantum confinement. Accounts of Chemical Research, 33(11) (2000) 773-780.

14. Chen, R. and Persson, C. Band-edge density-of-states and carrier concentrations in intrinsic and p-type CuIn1− x Ga x Se2. Journal of Applied Physics, 112(10) (2012) 103708.

15. Lue, J.T. Physical properties of nanomaterials. Encyclopedia of nanoscience and nanotechnology, 10(1) (2007)1-46.

16. Cuenot, S., Frétigny, C., Demoustier-Champagne, S. and Nysten, B. Surface tension effect on the mechanical properties of nanomaterials measured by atomic force microscopy. Physical Review B, 69(16) (2004) 165410.

17. Moradmard, H., Shayesteh, S.F., Tohidi, P., Abbas, Z. and Khaleghi, M. Structural, magnetic and dielectric properties of magnesium doped nickel ferrite nanoparticles. Journal of Alloys and Compounds, 650 (2015) 116-122.

18. Sta, I., Jlassi, M., Kandyla, M., Hajji, M., Koralli, P., Krout, F., Kompitsas, M. and Ezzaouia, H. Surface functionalization of sol–gel grown NiO thin

films with palladium nanoparticles for hydrogen sensing. international journal of hydrogen energy, 41(43) (2016) 291-3298.

19. G.M. Whitesides, et al., Molecular self-assembly and nano chemistry: a chemical strategy for the synthesis of nanostructures, Science 254 (1991) 1312.

20. W. Reddick and G. Amaratunga, Silicon surface tunnel transistor, Appl. Phys. Lett., 67(4) (1995) 494–496.

21. H. S. Lee, W. S. Um, K. T. Hwang, H. G. Shin, Y. B. Kim, and K. H. Auh, Ferroelectric properties of $Pb(Zr,Ti)O_3$ thin films deposited on annealed IrO_2 and Ir bottom electrodes, Journal of Vacuum Science and Technology A, 17(5) (1999) 2939–2943.

22. D.W, Johnson American Ceramic Society, Advances in ceramics: Ceramics Powder Science, Westerville, 21 (1987) 3-19.

23. Rasmussen, J.W., Martinez, E., Louka, P. and Wingett, D.G. Zinc oxide nanoparticles for selective destruction of tumor cells and potential for drug delivery applications. Expert opinion on drug delivery, 7(9) (2010) 1063-1077.

24. E. Kanazawa, G. Sakai, K. Shimanoe, Y. Kanmura, Y. Teraoka, N. Miura, N. Yamazoe, Metal oxide semiconductor N2O sensor for medical use. Sens. Actuat. B: Chem. 77 (2001) 72–77.

25. U. Kumar, S. Sikarwar, R. K. Sonker, B.C. Yadav, Carbon Nanotube: Synthesis and Application in the Solar cell, J. of Inorganic and organometallic polymers and material, 26(6) (2016) 1231-1242.

26. T.V. Duncan, Applications of nanotechnology in food packaging and food safety: Barrier materials, antimicrobials and sensors, Journal of Colloid and Interface Science 363 (2011) 1–24

27. Bhalla, A.S., Guo, R. and Roy, R. The perovskite structure-a review of its role in ceramic science and technology. Materials Research Innovations, 4(1) (2000) 3-26.

28. Tanaka, H. and Misono, M. Advances in designing perovskite catalysts. Current Opinion in Solid State and Materials Science, 5(5) (2001) 381-387.

29. Muller, O. and Roy, R.. The Major Ternary Structural Families, Springer, Berlin Heidelberg New York (1974).

30. B.C. Yadav, S. Singh, A. Yadav, Nanonails structured ferric oxide thick film as room temperature liquefied petroleum gas LPG sensor, Applied Surface Science, 257 (2011) 1960-1966.

31. F. He, Q. Huang, M. Qin, A silicon directly bonded capacitive absolute pressure sensor. Sens. Actuator A: Phy., 35 (2007) 507–514.

32. C.T. Huang, C.L. Shen, C.F. Tang, S.H. Chang, A wearable yarn-based piezoresistive sensor. Sens. Actuator A: Phy., 141(2) (2008) 396–403.

33. C.V.G. Reddy, S. V. Manorama, V.J. Rao, Preparation and characterization of ferrites as gas sensor materials, J. Mater. Sci. Lett. 19 (2000) 775-778.

34. C. Peng, Principle and Application of Biomedical Sensors, Higher Education Press, Beijing, China, (2000) 157–160.

35. L.A. Mercante, V.P. Scagion, F.L. Migliorini, L.H.C. Mattoso, D.S. Correa Electrospinning-based (bio) sensors for food and agricultural applications: A review, Trends in Analytical Chemistry 91 (2017) 91-103.

36. M.A. El Romb, D. Fasquelle, S. Deputier, M. Mascot, Elaboration and characterization of doped barium titanate films for gas sensing, AIP Conference Proceedings 1627 (2014) 25.

37. S. K. Hodak, T. Supasai, A. Wisitsoraat and Jose H. Hodak, Design of low-cost gas sensor based on SrTiO3 and BaTiO3 Films, J. of Nanosci. and Nanotechno. 10 (2010) 7236-7238.

38. K. Park, D.J. Seo, Gas sensing characteristics of BaTiO3-based ceramics, Mater. Chem. Phys. 85 (2004) 47-51.

39. J.J. Urban, W.S. Yun, Q. Gu, H. Park, Synthesis of Single-Crystalline Perovskite Nanorods Composed of Barium Titanate and Strontium Titanate, J. Am. Chem. Soc. 9 124(7) (2002) 1187.

40. M.R.A. Bhuiyan, M.M. Alam, M.A. Momin, M. J. Uddin, M. Islam, Synthesis and Characterization of Barium titanate (BaTiO3) nanoparticle, Int. J. of Mat. and Mechanical Engineering 1 (2012) 21-24.

41. O. Harizanov, A. Harizanova, T. Ivanova, Formation and Characterization of sol-gel barium titanate, Mat. Sci. and Engineering B 106 (2004) 191-195.

42. A. Kareiva, S. Tautkus, R. Papalaviciute, Sol-gel synthesis and characterization of barium titanate powders, J. of Mat. Sci. 34 (1999) 4853-4857.

43. H. Hayashi, T. Nakamura, T. Ebina, In-situ Raman spectroscopy of BaTiO3 particles for tetragonal–cubic transformation, Journal of Physics and Chemistry of Solids 74 (2013) 957–962.

44. P. Song, H.H. Zhang, D. Han, J. Li, Z. Yang, Q. Wang, Preparation of biomorphic porous LaFeO3by sorghum straw-biotemplate method and its acetone sensing properties, Sens. Actuators B: Chem., 196 (2014) 140–146.

45. H. Zhang, P. Song, D. Han, Q. Wang, Synthesis and formaldehyde sensing performance of LaFeO3 hollow nanospheres, Physica E 63 (2014) 21–26.

46. H. Xiao, C. Xue, P. Song, J. Li, Q. Wang, Preparation of porous LaFeO3microspheres and their gas-sensing property, Applied Surface Science 337 (2015) 65–71.

47. X. Ge, Y. Liu, X. Liu, Preparation and gas sensitive properties of LaFe1-YCoYO3 semiconducting materials, Sens. Actuators B: Chem., 79 (2001) 171-174.

48. Q. Peng, B. Shan, Y. Wen, R. Chen, Enhanced charge transport of LaFeO3 via transitionmetal (Mn, Co, Cu) doping for visible light photoelectron chemical water oxidation, International journal of hydrogen energy 40 (2015) 15423-15431.

49. R. Lu, J. Yuan, H. Shi, B. Li, W. Wang, D. Wang, M. Cao, Morphology-controlled synthesis and growth mechanism of lead-free bismuth sodium titanate nanostructures via the hydrothermal route, Cryst Eng Comm, 15, (2013) 3984–3991.

50. T. Yu, K.W. Kwok, H.L.W. Chan, Preparation and properties of sol–gel-derived Bi0.5 Na0.5 TiO3 lead-free ferroelectric thin film, Thin Solid Films 515 (2007) 3563– 3566.

51. L. A. Patil, D. N. Suryawanshi, I. G. Pathan, D.G. Patil, Effect of firing temperature on gas sensing properties of nanocrystalline perovskite BaTiO3 thin films prepared by spray pyrolysis techniques, Sens. Actuators B: Chem., 195 (2014) 643-650.

52. G.H. Jain, L.A. Patil, U.P. Mulik, K.R Patil, studies on gas sensing performance of pure and modified barium strontium titanate thick film resistors, Bull. Mater. Sci. 30(1) (2007) 9-17.

53. V.R. Chinchamalatpure, S.A. Ghosh, G.N. R. Chaudhari, Synthesis and Electrical Characterization of BaTiO3 Thin Films on Si(100), Materials Sciences and Applications, 1 (2010) 187-190.

54. B.D. Stojanovic, A. Z. Simoes, C. O. Paiva-Santos, C. Jovalekic, V.V. Mitic, J.A. Varela, Mechanochemical synthesis of barium titanate, Journal of the European Ceramic Society 25 (2005) 1985–1989.

55. D. Lakshmi, V. M. Priya, J. Shanthi, International journal of information technology & computer sciences study of barium titanate thin films by spin coating technique, 2(1) (2014) 301-303.

56. S. Katlakunta, P. Raju, S. S. Meena, S. Srinath, R. Sandhya, P. Kuruva, S.R. Murthy, Multi ferric properties of microwave sintered $BaTiO_3$–$SrFe_{12}O_{19}$ composites, Physica B, 448 (2014) 323–326.

57. K. Suresha, T.S. Panchapagesan, K.C. Patil, Synthesis and properties of La1xSrxFeO$_3$, Solid State Ionics 126 (1999) 299-305.

58. M. Rawat, K. L. Yadav, A. Kumar, P. K. Patel, N. Adhlakha, J. Rani, Structural, dielectric and conductivity properties of Ba2+ doped (Bi0.5 Na0.5)TiO3 ceramic. Adv. Mat. Lett. 3 (4) (2012) 286-292.

59. V. R. Mudinepalli, N. R. Reddy, W. C. Lin, K.V. Siva Kumar, B.S. Murty, Phase transitions of the ferroelectrics (Bi0.5 Na0.5)TiO3by dielectric and internal friction measurement. Adv. Mater. Lett. 6(1) (2015) 27-32.

60. K.K. Bhargav, A. Maity, S. Ram, S.B. Majumder, Low temperature butane sensing using catalytic nano-crystalline lanthanum ferrite sensing element, Sensors and Actuators B. 195 (2014) 303–312.

CHAPTER 2

SYNTHESIS AND CHARACTERIZATION TECHNIQUES

2.1 Synthesis Methods of Nanomaterials

There are several methods used for the preparation of nanomaterials over a range of sizes, shape, chemical compositions and physicochemical behavior, and have seen a vast advances and modifications over the time. The varieties of such methods are divided broadly into two categories [1].

(a) Bottom-up Approach/ Chemical Methods

(b) Top-down Approach/ Physical Methods

Classifications of synthesis methods are schematically illustrated in following **Figure 2.1**

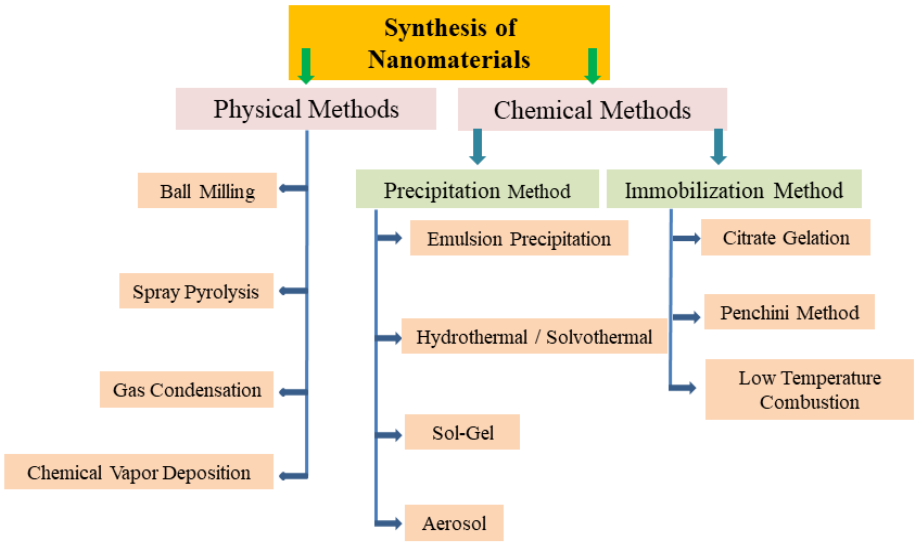

. **Fig. 2.1:** Classification of the synthesis methods

2.1.1 Chemical methods

The chemical method gives over other, the excellent chemical homogeneity. It happens because of the mixing at molecular level for synthesis using chemical route. The principal advantage of this method is the control over the surface area and size of nanomaterials. Some of the chemical methods are as:

2.1.1.1 Precipitation method

(a) Emulsion precipitation method

(b) Hydrothermal/Solvothermal method

(c) Aerosol method

(d) Sol-gel method

In all these methods, nanoparticles are found to be in the form of a precipitate.

2.1.1.2 Immobilization Method

(a) Citrate gelation method

(b) Penchini method

(c) Low temperature combustion method

2.1.1.1.1 Emulsion Precipitation Method

This method requires the formation of durable emulsion systems, which is possible with the addition of surfactant to water-oil system. Small numbers of atoms added in the emulsion system. The stable precipitate formed by the exchange of reactive species between the droplets of the emulsion. According to Einstein-Smoluchowski equation, the identical exchange rate between the droplets is slower than the normal rate of particle growth. So, the mechanisms of nucleation and growth for this method are retarded in compare with those for homogeneous solution, quitting

formation of the large particles. To form a thermally stable emulsion and to control the droplet size, multi surfactants are very much capable.

This synthesis method comes up with the specific advantage that it prevents agglomeration of particles which are formed in individual bubbles. Further it makes feasible subsequent synthesis routes at remarkably low temperature [2].

2.1.1.1.2 Hydrothermal/ Solvothermal Synthesis

The hydrothermal reaction is also known as thermal hydrolysis or hydrothermal hydrolysis. In the hydrothermal process, the aqueous reaction is carried out in an autoclave or high-pressure reactors (2000 psi) and high temperature ranging from 100-300 ºC. In this process, water is used to accelerate the kinetics and act as a reactor for the hydrolysis reaction. Alkali and acid used as a pseudo catalyst during the process. The sol of metal hydroxide or metal oxide is made from aqueous solution at lofty temperature and pressure.

The hydrothermal reaction is a step by step procedure of the following sub process which is given as under:

1. Oxidation
2. Precipitation
3. Deoxidization
4. Decomposition
5. Crystallization

The basic advantage of hydrothermal method in comparison with other type of crystal growth is that it has the capability to create the crystalline phases that are not lasting at melting point. Also the materials, those having high vapor pressure nearby their melting points can be generated by this synthesis method. The method is exceptionally suitable for growth of great good-quality crystals when maintaining

good control upon their composition. The limitations of this mechanism are that there is a need of expensive autoclaves and there is an impossibility to observe the crystal when it grows.

2.1.1.1.3 Sol-Gel Method

The most common method of synthesis of nanomaterial in the desired shape like a flower, fibre thin-film, etc., is obtained by sol-gel method. It is very simple and cheap method which widely used for the synthesis of the material. "Colloidal" is the solid particle ranging from 1-100 nm range. "Sol" produced by dispersing colloidal solution in the liquid. An intermediate structure formed by polymeric chain and pores are known as "Gel." Regular precursors are metal alkoxides and metal chlorides, which are gone through different forms of hydrolysis and poly-condensation reactions [3-4]. Formation of sol takes place by dissolving alkoxide, inorganic metal salt into a suitable solvent. After continuous stirring, a homogeneous mixture achieved. The two important reactions that occur in this process is hydrolysis followed by condensation of metal [5]. Usually, an alcoholic solvent used for dissolving alkoxide.

M-OR + H_2O → M-OH + ROH Hydrolysis

M-OH + OR-M → M-OM +H_2O Condensation

The sol obtained after hydrolysis and condensation is low viscous liquid. Spin coating, dip coating and screen printing methods are further used for the fabrication of the thin films. **Figure 2.2** shows the mechanism of sol-gel process.

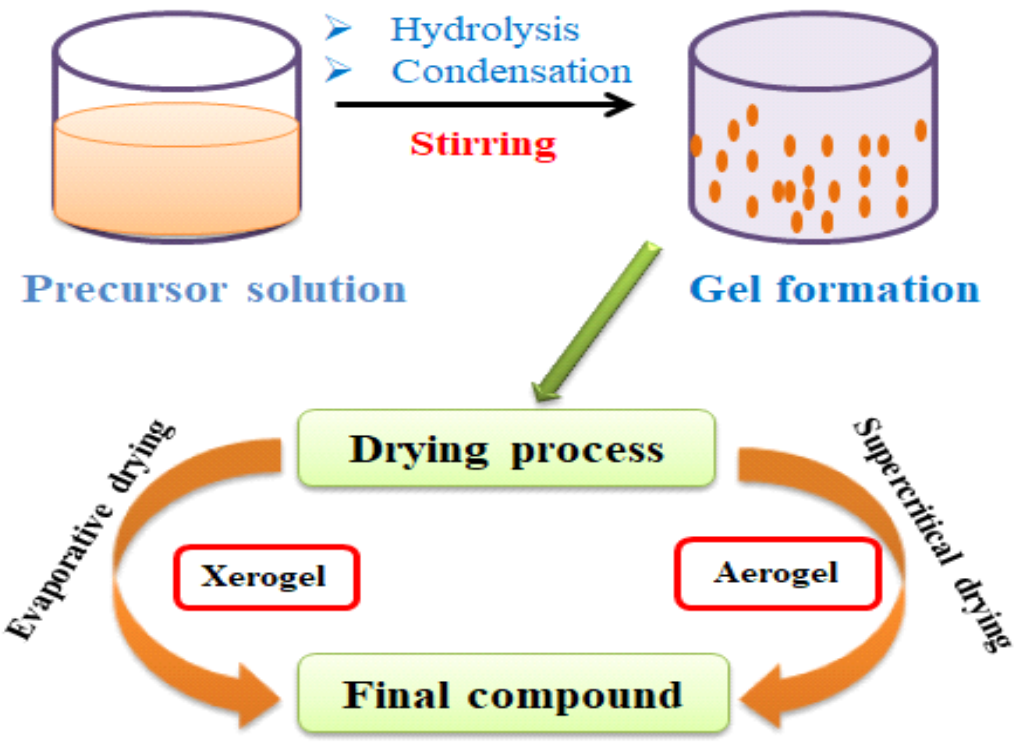

Fig. 2.2: Schematic of the sol-gel synthesis technique

2.1.1.2 Immobilization Method

2.1.1.2.1 Citrate Gelation Method

In citrate gel method, the aqueous precursor is used for the synthesis of nanoparticles. The organic network is formed when metal ions are dissolved and stabilized in precursor solutions. After heat treatment, fine metal oxide particles are obtained. Citrate method is basically used for the preparation of multi-component compositions. They have the ability to prepare multi-component with homogeneous structure. Poly chelates are formed between the ligands of citric acid and metal ions. On heating, these poly chelates poly-esterification occurs with polyfunctional alcohol. Evaporation of the precursor containing metallic salts and citric acid shows an important role in poly chelation process. A viscous resin and a transparent glassy gel are obtained after heat treatment. Initially, Immobilization of different metal ions

takes place from the mixture to form a rigid system to avoid the risk of segregation into different oxide compositions after calculations [6].

2.1.1.2.2 Penchini Method

The process of the Penchini is same as the Citrate-gel method in which metal nitrates are dissolved in alcohol instead of citrate.

2.1.2 Physical Methods

There are different physical methods which are presently in practice for the synthesis and commercial production of nanomaterials. Some physical methods are given below:

2.1.2.1 Ball Milling

In the late 1960, Benjamin and his co-workers developed this process. In ball milling, the mixture of powder is kept inside a chamber containing metallic balls. Fine, uniformly dispersed metal oxide nanoparticles are synthesized by mechanical alloying in ball milling method. Beside synthesis, high energy produced while ball milling is used to change chemical properties by modifying the reactivity of milled solid. These planetary balls are used for providing high energy to the solid salt and for mechanical alloying. Attritor planetary ball, horizontal ball mill are the apparatus used in this alloying process [7]. This method is mostly used in laboratories. The milling system contains a rotating disc and a bowl opposite to the direction of the disc for synchronizing centrifugal forces, powder mixture, surfactant, rotating the ball. The mixture of the powder is fractured and cold welded under high energy impact. These metallic balls are of used for high-speed milling and these balls are called the planetary ball. In the initial stage, the powder is partially flattered due to the collision of balls. In the intermediate stage, metastable structure is obtained by mechanical alloying process occurs followed by fracturing and cold welding process. In the final

stage reduction and refinement in particle size is done. Thus, a nanomaterial is fabricated. **Figure 2.3** shows the ball milling method with rotation of disc in opposite direction with planetary ball.

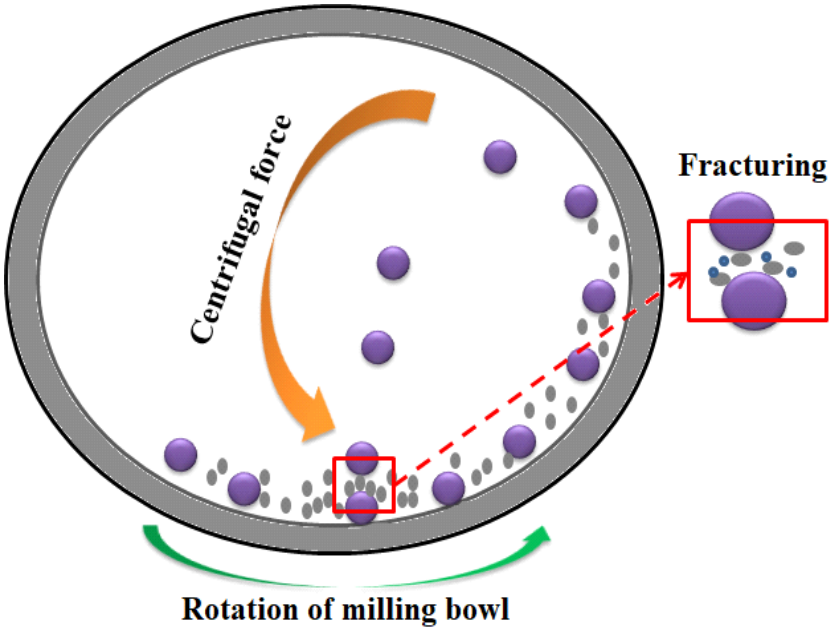

Fig.2.3: Schematic diagram of ball milling method

2.1.2.2 Spray Pyrolysis

Pyrolysis includes spray pyrolysis, aerogel pyrolysis, and laser-assisted pyrolysis. Spray pyrolysis is also called aerogel pyrolysis or vapour pyrolysis. There is a minor difference between spray pyrolysis and aerogel pyrolysis in the delivery of the reactant on the substrate. The main parts of the aerogel pyrolysis instrument are:

(i) Generator, to obtain aerogel state from the liquid

(ii) Furnace for particle formation

(iii) Particle collector

(iv) Flow meter to check the flow rate

In aerogel, pyrolysis nanoparticles are used in vapour form to deliver it in the hot reactor while in spray pyrolysis these are in the small droplets form which directly delivered from the nebulizer. Metal ions are dissolved in the aqueous solution

to form a homogeneous precursor. This precursor is converted in aerogel in presence of oxygen, nitrogen or mixture of gases. Size dependency varies in aerogel by type of generator used, the volume of carrying gas and nature of the liquid. The formed aerosol is then carried inside the electric furnace where liquid droplets go through evaporation, solute precipitation, solute decomposition and finally sintering of oxide [8-9].

The nanomaterial obtained via this process is spherical in shape with minimal agglomeration, which is good for gas sensing applications. Major disadvantage of this method is the large size distribution of nanoparticles and requirement of large amount dilution for carrying gas to avoid cluster formation.

2.1.2.3 Sputtering

Sputtering is the physical process in which high-energy projectile particles are used for the ejection of the particle from matter target by transfer of momentum. John Thornton and Joseph Greene have described deposition technique method by the sputtering phenomenon. Sputtering deposition in a stable plasma system permits extremely good control on deposition rate which is proportional to the discharge current between the electrodes and the number of atoms ejected or sputter yield of the cathode material. Sputter yield is defined as the ratio of the mean of emitted number of atoms to the incident atoms [10]. **Figure 2.4** represents the schematic diagram for this method.

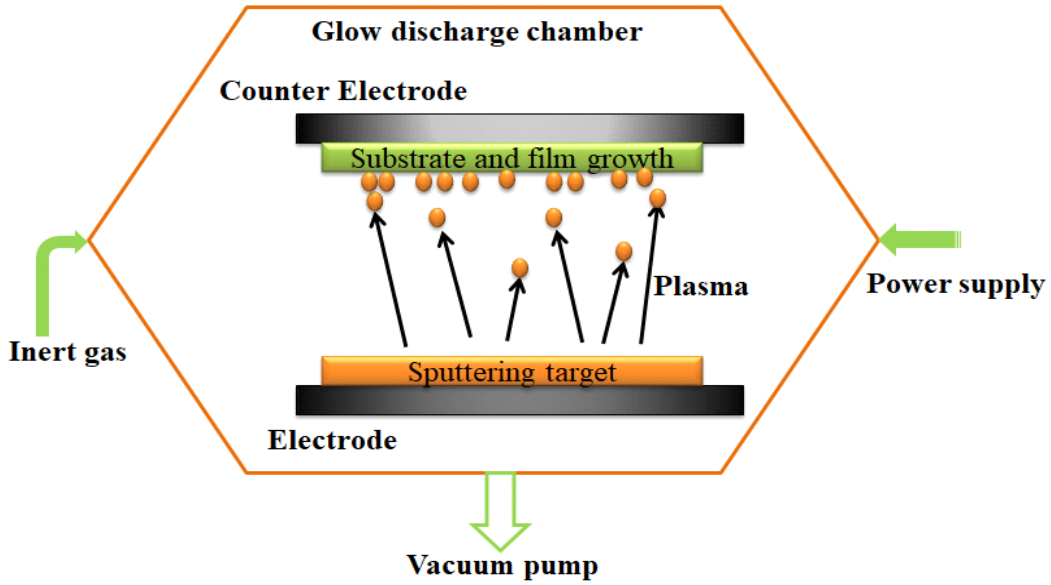

Fig.2.4: Schematic diagram of sputtering

Based on the deposition technique sputtering is divided into following categories:

1. Diode Sputtering
2. Reactive Sputtering
3. Bias Sputtering (Ion Implantation)
4. Magnetron Sputtering
5. Ion Beam Sputtering Depositions
6. Reactive Ion Implantation
7. Cluster Beam Deposition

2.1.2.4 Chemical Vapor Deposition (CVD)

Chemical vapor deposition (CVD) is a chemical process which is used to produce highly pure solid materials. It is the most reliable method for synthesis of nanomaterial. In this technique nucleation of particles in the vapour state takes place rather than the deposition of the film. The process is used to make a very thin film and is used in electronic industry and semiconductor industry. In a typical CVD process, the wafer (substrate) is exposed to one or more volatile reactant gases usually called

precursors. When come into contact with the substrate, precursors react and/or decompose on the substrate surface to produce the desired deposit and when the mixture of gas reactant is inserted inside the reacting chamber and chemical reaction among the gas molecule take place. **Figure 2.5** shows the simple schematic diagram of CVD mechanism.

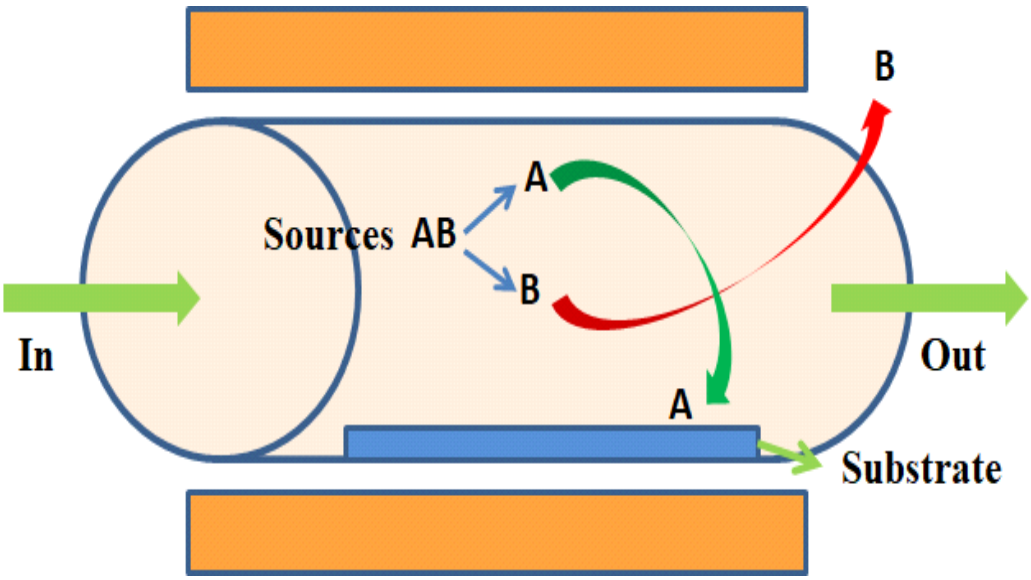

Fig.2.5: Simple schematic diagram of CVD mechanism

Chemical reaction types include pyrolysis (thermal decomposition), hydrolysis, oxidation, reduction, synthesis reactions, nitride and carbide formation, disproportionation, and chemical transport [11]. CVD can be classified into further as:

1. Chemical Vapour Deposition (CVD)
2. Plasma Enhanced chemical vapour deposition (PE-CVD)
3. Metal-Organic chemical vapour deposition (MO-CVD)
4. Atmospheric pressure chemical vapour deposition (AP-CVD)
5. Low-pressure chemical vapour deposition (LP-CVD)
6. Ultrahigh vacuum chemical vapour deposition (UHV-CVD)
7. Aerosol-assisted chemical vapour deposition (AA-CVD)
8. Direct liquid injection chemical vapour deposition (DLICVD)

2.2 Characterization Techniques

The characterization of nanomaterials is very important aspect to understand their structure, chemical composition, properties and applications. This section focuses on instruments and experimental methods employed towards the characterization of the synthesized materials such as X-ray Diffraction analysis (XRD), Scanning Electron Microscopy (SEM), Transmission Electron Microscope (TEM), Fourier Transform Infrared Spectroscopy (FTIR), EDX and other techniques.

2.2.1 Scanning Electron Microscopy

The SEM machinery system with different detectors can serve the following facilities:

- Images of high-resolution
- Elemental analysis of bulk material
- Speedy elemental mapping
- Compositional, topographical and other information
- Detection for small variations of trace element
- Imaging and analysis of those samples in both natural and hydrated state
- Digital output

When a beam of electrons impinges on a solid surface, it undergoes numerous interactions at the solid surface depending on the incident beam. The incident electrons are transmitted, absorbed, scattered or reflected. The outgoing beams from the sample consist of electrons, X-rays, visible-IR photons. Each of these signals contains information about the surface conditions, compositions, structural defects and impurity contents of the sample [12]. **Figure 2.6** shows the mechanism of scanning electron microscope.

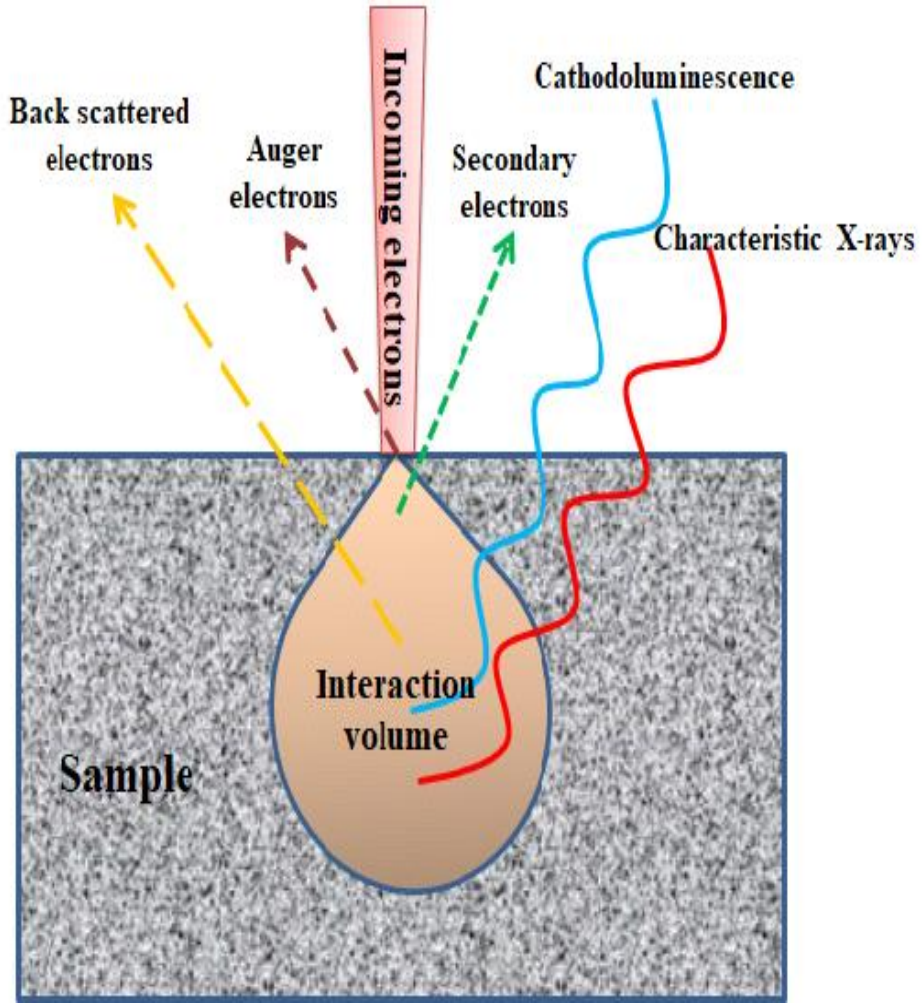

Fig. 2.6: Scanning electron microscope mechanism

2.2.2 X-ray Diffraction Analysis

X-ray diffraction analysis is a multifaceted, non-destructive approach that reveals extensive knowledge regarding the chemical composition and the crystallographic structure of the natural and constructed materials [13]. Monochromatic X-rays are applied for determining the interplanar spacing's of the synthesized unfamiliar materials. Samples are analyzed in powdery form with grains in arbitrary orientations to confirm that every crystallographic direction is examined by the X-ray beam. So, when the condition of constructive interference is fulfilled by Bragg's law, reflection is produced and heights of the relative peaks are usually

proportional to the grains number in preferred orientation. **Figure 2.7** represents Bragg's law of X-ray diffraction study.

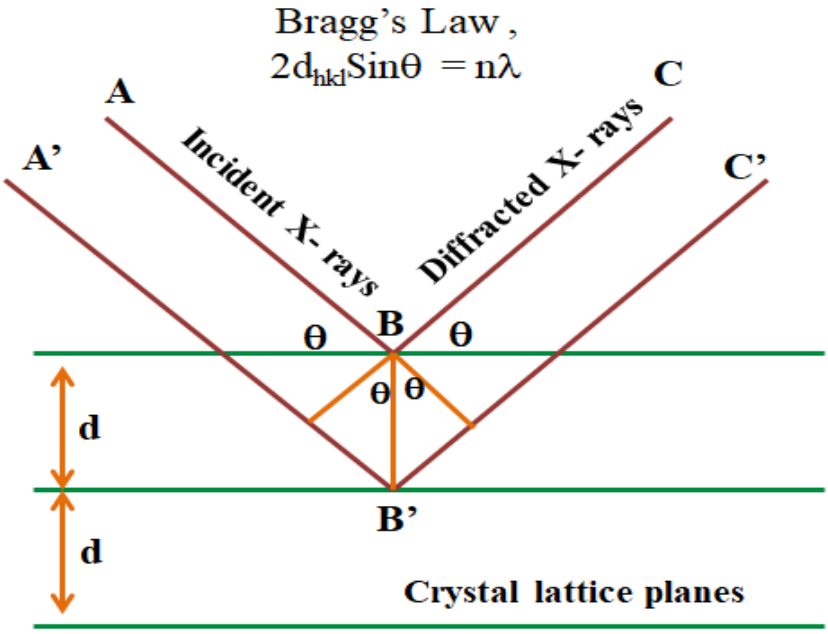

Fig. 2.7: Bragg's law of X-ray diffraction

2.2.3 Fourier Transform Infrared Spectroscopy

This (FTIR) is a widespread characterization technique to reveal the frequency of vibrational stretching of metal-oxygen bonds. Generally, the aim of this spectroscopy is to determine how definitely a particular sample can absorbs or transmits the light at every variant wavelength. To use this spectroscopy, we use a continuous source of light to make a broad range of light of infrared wavelengths. The principle work of this method is to detect the infrared (IR) reflection and absorption features over the broad spectral region. FTIR used with the basic goal of determining changes in the intensity of infrared light as it interacts with material as a function of wavelength. This technique can give information on the chemical bonding in a material and is also non-destructive [14]. In FTIR analysis there are three commonly examined pieces of data. Those are the position of peak, the width of peak and the intensity of peak.

When infra-red beam enters in the sample as shown in **Figure 2.8**, it can be reflected, transmitted, or absorbed. The infra-red energy which is reflected from the surface is generally lost. So when the beam of infra-red light is passes through a particle, it can reflect off next particle or it can be transmitted through next particle. The infra-red energy after scattering is gathered by spherical mirror which is focused to the detector. These are basics of how the diffuse reflectance mode of the FTIR works. **Figure 2.8** shows the mechanism of FTIR spectroscopy.

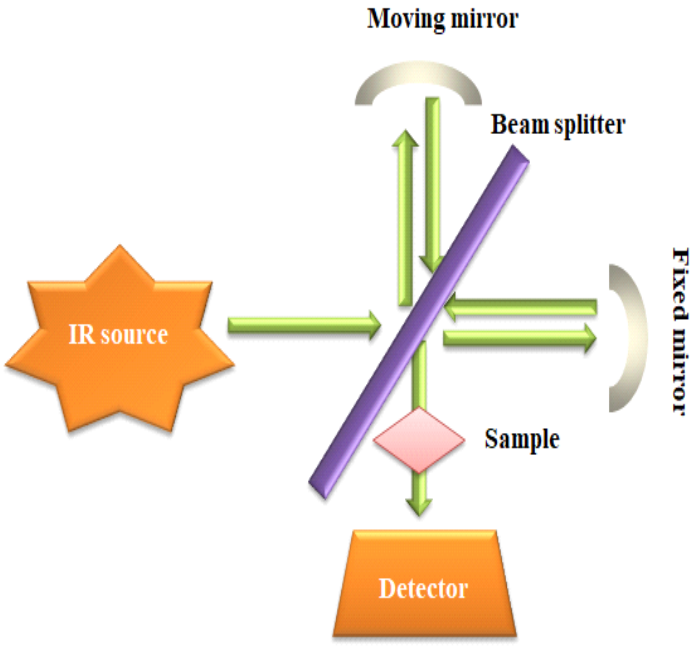

Fig. 2.8: Mechanism of FTIR

2.2.4 Ultraviolet-Visible Spectroscopy

Ultraviolet-visible spectroscopy denotes to the absorption spectroscopy in the region of UV-visible range. It means this spectroscopy uses the range of light in visible and adjacent (i.e. near-UV and near-infrared) areas. This absorptive property directly has an effect on the colour of chemicals involved. In this particular region of EM spectrum, electronic transitions occur in molecules. Fluorescence spectroscopy is a complementary technique with it. Because, in fluorescence, transition is occurred from excited to ground state, which is opposite to absorption mechanism.

The instrument for ultraviolet-visible spectroscopy is termed as UV/Vis spectrophotometer. It can detect the intensive light which is passing through sample (I) and then it compares the intensity of light without presence of sample (I_0). So, we can calculate transmittance which is the ratio of I_0/I and it is usually termed as percentage transmittance (%T). The absorbance, A, depend on transmittance as follow:

$$\boldsymbol{A = -\log(\frac{\%T}{100})} \text{ - - - (2.1)}$$

The change in absorption coefficient as function of photon energy for direct transitions which are allowed is as follows:

$$\boldsymbol{\alpha = A\,(h\nu - E_g)^{1/2}} \text{ - - - (2.2)}$$

In equation (2.2), α, is acquired from Beer's law which defines the absorption coefficient; A is constant; h denotes the Plank's constant; ν represents the frequency and E_g illustrates the energy of band gap between valence and conduction band.

$$\boldsymbol{I = I_o \exp(-\alpha x)} \text{ - - - (2.3)}$$

In above equation, x measures the thickness of evaluated sample. The variation of α^2 with photon energy was used to get the value of direct band gap energy with extrapolation of the linear tangential portion of the curve at zero absorption line. **Figure 2.9** represents different energy band gap.

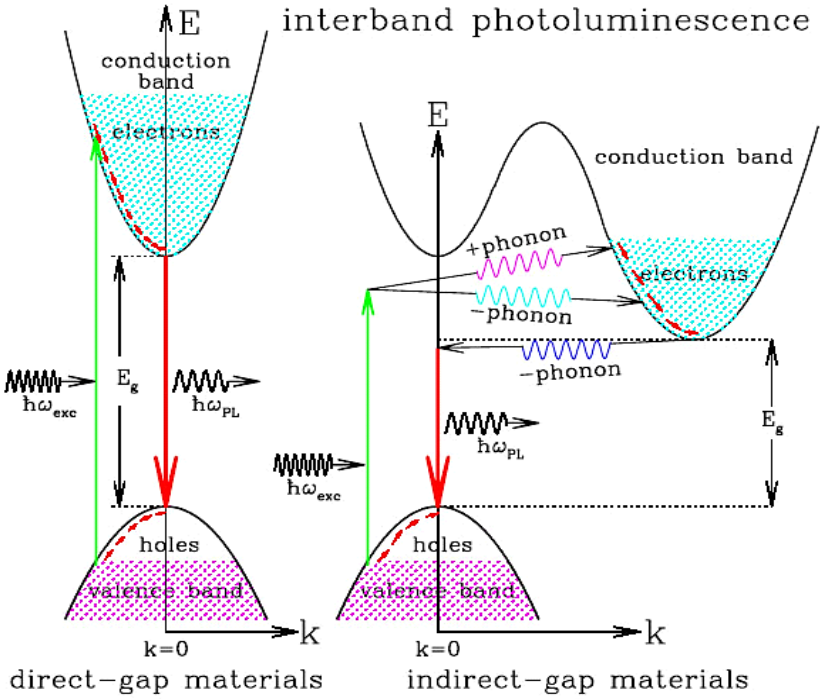

Fig. 2.9: Different band gap of materials [15]

2.2.5 Transmission Electron Microscopy

Transmission Electron Microscope (TEM) is a microscope generally used to magnify image of an ultra-thin specimen. The high-resolution magnified image contains information about the constitutional characteristics of the material. In this method, electron beams are allowed to pass through a specimen. While passing through it interacts with the specimen and produces an image. Then the imaging device, the fluorescent monitor magnifies and focuses the images to a layer of photographic film or recorded or detected by a charge-coupled sensor.

TEMs are more efficient in working than the light microscopes. Generally it is having higher resolution capacity than light microscopes as because it comprises of the small de Broglie wavelength of electrons. Presence of this small de Broglie wavelength of electrons makes the instrument highly sophisticated and thus supports to observe very small objects like a single column of atoms, which in general a thousand times smaller than the minimum resolving capacity of an object by a light microscope. This helps the application of TEM in different fields like materials

science, nanotechnology, semiconductor research in addition to population, virology, and cancer research.

(a) Sample preparation

In general, it is a complex and tedious work to prepare samples for analysis in TEM. The size or thickness of the prepared TEM samples must be in nanometres not like XRD or neutron where samples are directly exposed to electron beam as a result it increases the atomic number squared (z^2). Samples having higher quality will have a thickness of about 10 nanometres that is equivalent with the electrons mean free path when they are travelling through the samples. Usually, the samples are likely to be resistant naturally towards vacuum in metallurgy and material science research even though the samples should be made like a thin film or as a thin foil or carved any part of the sample so that electron can easily infiltrate through it.

Limitations

TEM method is highly delicate, efficient and sensitive but it is having some disadvantages like to make the sample like a thin film the materials have to go through wide process of sample preparation. The sample has to be thin enough to penetrate the electron beams. So in overall, TEM study is extensively time consuming process with a little output. Besides, during the preparation of sample, sample structure can also be altered. Again the field observation is comparatively lesser and increasing the possibility that the analyzed area may not be entirely characteristic of the entire sample. Mostly in the analysis of biological samples, there is a potential possibility of sample spoilage due to the application of electron beam. **Figure 2.10** shows the schematic diagram of TEM.

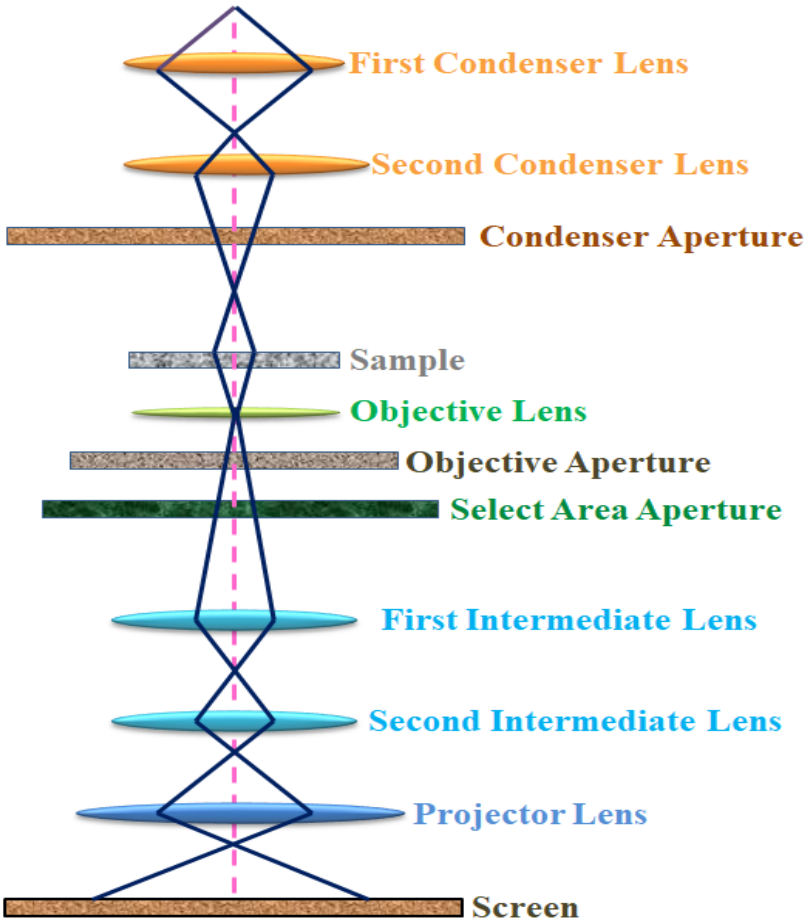

Fig. 2.10: Schematic diagram of TEM.

References:

1. K. Kimura, in “Fine Particles: Synthesis and characterization and Mechanism of Growth” (Sugimoto Tadao, Ed.), Marcel Dekker, New York, (2000) 513.
2. Woudenberg, F. C., Sager, W. F., Sibet, N. G., & Verweij, H. Dense nanostructured t-ZrO2 coatings at low temperatures via modified emulsion precipitation. Advanced materials, 13(7) (2001) 514-516.
3. M. Zayat, D. Levy, Blue CoAl2O4 particles prepared by the sol-gel and citrate gel methods, Chem. Mater., 12 (2000) 2763-69.
4. L.L. Hench and J.K. West, The sol-gel process, Chem. Rev. 90 (1990) 33-72.
5. A.E. Gash, T.M. Tillteson, J.H. Satcher, L.W. Hrubesh and R.L. Simpson, New sol-gel synthetic route to transition and main group metal oxide aero-gels using inorganic salt precursors, J. Non-Cryst. Solids 285 (2001) 22-28.
6. M. Zayat, D. Levy, Blue CoAl2O4 particles prepared by the sol-gel and citrate gel methods, Chem. Mater., 12 (2000) 2763-69.
7. O.K. Tan, W. Cao, Y. Hu, W. Zhu, Nanostructured oxides by high-energy ball milling technique: application as gas sensing materials, Solid-State Ionics 172 (2004) 309-331.
8. Tischner, T. Maier, C. Stepper, A. Köck, Ultrathin SnO2 gas sensors fabricated by spray pyrolysis for the detection of humidity and carbon monoxide. Sens. Actuat. B Chem. 134 (2008) 796–802.
9. A.M. More, J.L. Gunjakar and C.D. Lokhande, Liquefied petroleum gas (LPG) sensor properties of interconnected web-like structured sprayed TiO2 films, Sens. Actuators B 129 (2008) 671-677.
10. P.C. Zalm, Quantitative Sputtering, Surface and Interface Analysis, 11(2) (1983) 124.

11. K.L. Choy, Chemical vapour deposition of coatings. Prog. Mater. Sci., 48 (2003) 57–170.

12. M. Schenk, A.R. Reichelt, An electron microphone as a force sensor for combined scanning probe microscopy. Ultramicroscopy, 65 (1996) 109–118.

13. Hanawalt, J. D., Rinn, H. W., & Frevel, L. K. Chemical analysis by X-ray diffraction. Industrial & Engineering Chemistry Analytical Edition, 10(9) (1938) 457-512.

14. Smith, B. C. Fundamentals of Fourier transform infrared spectroscopy. CRC press (2011).

15. Li, A. Interaction of nanoparticles with radiation. arXiv preprint astro-ph/0311066 (2013).

16. Gao, P. X., Ding, Y., Mai, W., Hughes, W. L., Lao, C., & Wang, Z. L. Conversion of zinc oxide nanobelts into superlattice-structured nanohelices. Science, 309(5741) (2015) 1700-1704.

CHAPTER 3

SYNTHESIS AND CHARACTERIZATION OF BARIUM TITANATE ($BaTiO_3$) & ITS APPLICATIONS AS CO_2 SENSOR

3.1 Introduction

The first piezoelectric perovskite ceramic transducer is developed with isostructure using mineral perovskite is barium titanate ($BaTiO_3$) [1]. It is generally a ferroelectric perovskite ceramic which experiences three transitional stages with decrease in temperature. Transformation flows to shapes from cubic phase to tetragonal phase to orthorhombic and finally to rhombohedral phase [2-3]. In on and above the room temperature, $BaTiO_3$ is stable and shows ferroelectric properties by mechanical and chemical means.

Basically, the operational mechanism of conventional solar cell is based on the classical phenomenon of the p-n junction but there are some potent limitations like lattice disparity, band alignment etc. So that, ferroelectric photovoltaic cells are developed to astounded such limitations. As to rectify different behaviours and to increase the upright performance solar cell, $BaTiO_3$ is extensively used as it is very easy to roll in between the electrodes [4-5]. Additionally, $BaTiO_3$ is used as condenser material owing to their flat temperature characteristic curves. Condensers are used for coupling bi-pass and filter [6]. $BaTiO_3$ is porous in nature and this property helps the researchers to keep more concentration on different sensors like the ceramic gas sensor and humidity sensor. In general, ceramic gas sensors are categorized into two basic types which are 1) semiconducting ceramic gas sensor and 2) protonic gas sensor. The first type works on higher temperature (300-400 ^oC) and another one on

normal room temperature [7]. The functional mechanism of both the sensors is adsorption; in both the gas sensors gas molecules are being functionally adsorbed.

A perusal of the literature reveals that a lot of research work has been done on the synthesis, properties and applications of $BaTiO_3$ ceramic. Different techniques or methods can be employed for preparation of $BaTiO_3$, namely solid-state method, sputtering, hydrothermal, precipitation, laser ablation, vacuum evaporation, sol-gel method etc. [8]. On comparing all the techniques, sol-gel method has numerous advantages and is mostly used by the researchers these days. Basically it is a simple and flexible technique where an alkaloid is used for dissolving a solute then hydrolysed followed by polycondensation to form a sol and then to a gel [9]. In the present study, sol-gel method was used for synthesizing perovskite type $BaTiO_3$. A glass was used as substrate for fabrication of a thin film in the process. After comprehensively characterizing, in the range of 100 to 1300 ppm concentration of CO_2 gas, it was employed as CO_2 sensor. After examining, the results were found more satisfactory over the existing described research work [10-11]. CO_2 is a hazardous gas. It is becoming a harmful gas to human health causing breathing problems because of its increasing concentration day-by-day. So it is very much important to identify the detection of CO_2 in the environment for human welfare. So researchers are trying to develop CO_2 sensor sensitive for the lower concentration [12]. The current research work deals with the CO_2 sensing.

3.2 Structure of Barium Titanate

Barium titanate retains a classic element cell ABO_3 configuration. Structure of perovskite shown in **Figure 3.1**, comprises a centre containing a transitional metal ion with corner allocation of O_6 octahedral ions. Empty d-shell consists of non-magnetic transition element to form majority of the ferroelectric perovskite. The non-magnetic

elements thus joined with adjacent oxygen ions by a covalent bond to form a molecule. A classic ABO_3 unit cell composed of a corner-linked network of oxygen octahedral with Ti^{4+} ion occupied in B sites with octahedral frame and Ba^{2+} ions situated in A sites formed by associated octahedral.

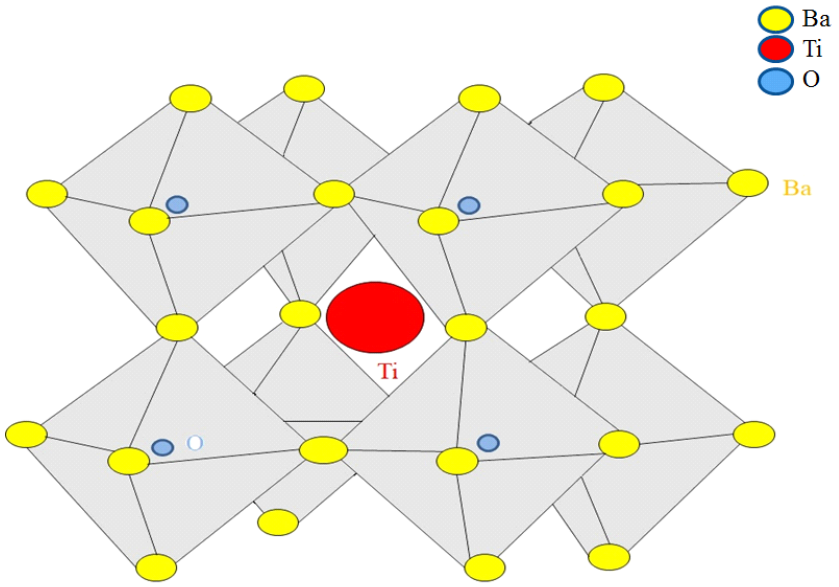

Fig. 3.1: Perovskite structure of $BaTiO_3$

3.3 Experimental Details

3.3.1 Materials

Barium chloride dihydrate ($BaCl_2.2H_2O$) and titanium tetrachloride, acetic acid, PEG.

3.3.2 Synthesis of Barium Titanate Powder

In this work, sol-gel method technique was employed to prepare the barium titanate [13]. The beginning materials are barium chloride dihydrate ($BaCl_2.2H_2O$) and titanium tetrachloride and methanol used as a solvent. Firstly, barium chloride dihydrate (2.4428 gm) was dissolved in methanol, and then separately prepared a solution of titanium tetrachloride (1.89679 gm). After that it was continuously stirred for 2 h. Then both the solutions are mixed together to make a stock solution. The stock solution again continuously stirred for 2 h to get a final sol of barium titanate

with addition of acetic acid. After that, PEG was added to get the gel of sol. Later on this gel was oven dried (100^{o} C) and then annealed (600^{o} C for 2h) in a programmable furnace to anneal the gel form of sample. After annealing, pestle and mortar was used for crushing to get a fine crystalline powder. Subsequently, to remove the impurities (e.g. chlorine) we further modified the process by washing with double deionized water. Then again we have done calcination to get modified form of barium titanate. The flow diagram of the barium titanate synthesis process is shown in **Figure 3.2**.

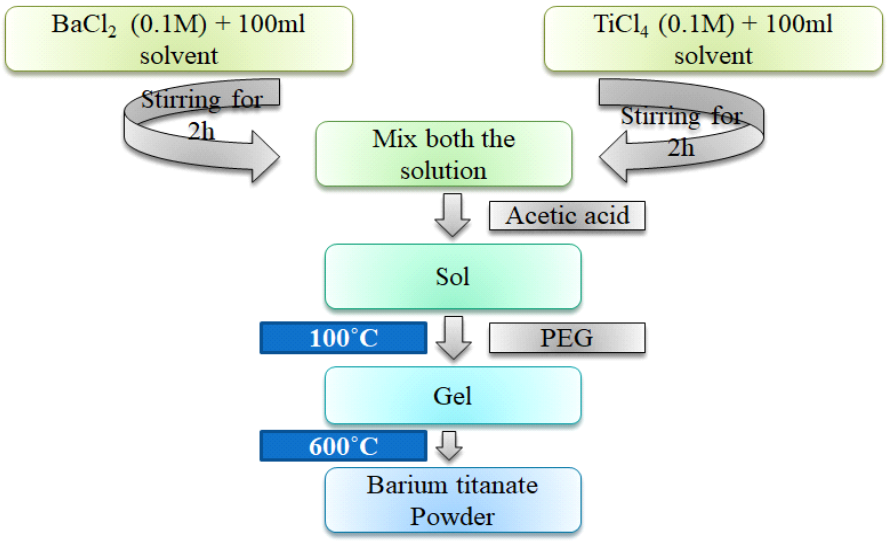

Fig. 3.2: Flow diagram for synthesis method

3.3.3 Preparation of Thin Film of Barium Titanate

To deposit the invariable thickness of thin film, among different type of techniques sol-gel spin coating method is the best method of coating. It is the best method for depositing uniform thickness of thin film [14]. To get that object, a glass substrate was prepared of 1×1 cm^{2} dimension and thoroughly cleaned with ultrasonic cleaner (WUC-AO2H) mixed with distilled water and ethanol and finally followed by acetone. Then a dense solution of BTO was prepared using acetic acid (1:3 ratios). This dense solution was kept in vigorous stirring for 2 h and followed by sonication for another 2 h. Then a glass substrate was used to spin the solution by using spinner (METREX RC100) at 3000 rpm for 40 s at 80^{o} C. Then it was dried on a hot plate for

10 min. The spin coating process followed by drying was repeated again. To obtain a homogenous thin film, the process was repeated twice more and finally the thin film was dried on hot plate at 80° C for 20 min and then annealed at 200° C for 2h.

3.3.4 Experimental Setup for CO_2 Sensing

Fabrication of barium titanate thin film was followed according to prescription illustrated as in section.3.3.3. After fabrication, the thin film was used as CO_2 sensor. Detailed description of the experimental setup shown in **Figure 3.3**, which comprises of different units such as cylinder of CO_2, gas flow meter, controlled gas chamber, hot plate, volume measuring unit and a Keithley electrometer model no. 6517 B.

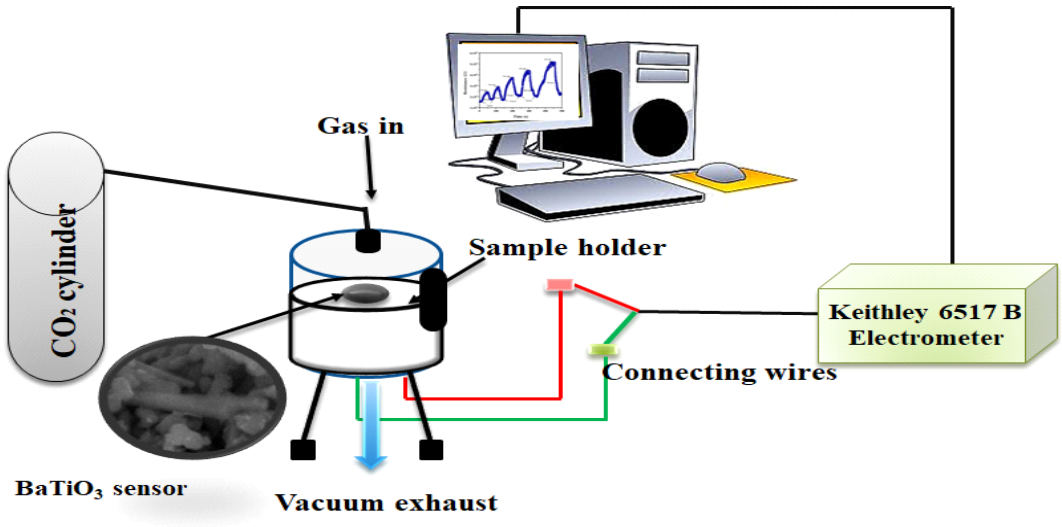

Fig. 3.3: Experimental set-up for sensing of CO_2

3.3.5 Characterization

For the determination of crystallinity of the prepared titanate, powder XRD pattern was recorded by glancing angle X-ray Diffractometer (Bench top X-ray Diffraction, 5th generation Miniflex), in which monochromatic Cu-Kα act as the source of radiation. SEM (Zeiss EV040) combined with EDX was employed to study the surface morphology of the material. TEM analysis was performed (by TECNAI 200 KV TEM (Fei, Electron Optics), AIIMS Delhi). UV-Visible spectrophotometer

(Evolution 201) was used for examining the optical properties of the sample. FTIR spectra was analyzed and documented by Thermo Nicolet (Model No. 6700, USIC) to test the prepared $BaTiO_3$.

3.4 Results and Discussion

3.4.1 X-ray Diffraction Analysis

The **Figure 3.4** represents the X-Ray diffraction pattern of synthesized nano-powder of BTO. We have analysed the XRD pattern and found a match with JCPDS no. 00-008-0372. The peaks at 2θ = 41.1418 (203), 44.4358 (204), 49.0018 (211), 64.964 (220) confirm the development of perovskite barium titanate [15]. The peaks at 2θ = 28.0546 (202), and 30.8118 (400) presents the peaks for β-TiO_2. These are found by matching with JCPDS no. 46-1238. Using Debye Scherer's equation we have calculated the minimum average crystallite size and it is 9.18 nm. The crystallites size of each peak was also calculated and it was found as 15.71 nm the average crystallite size [16-18].

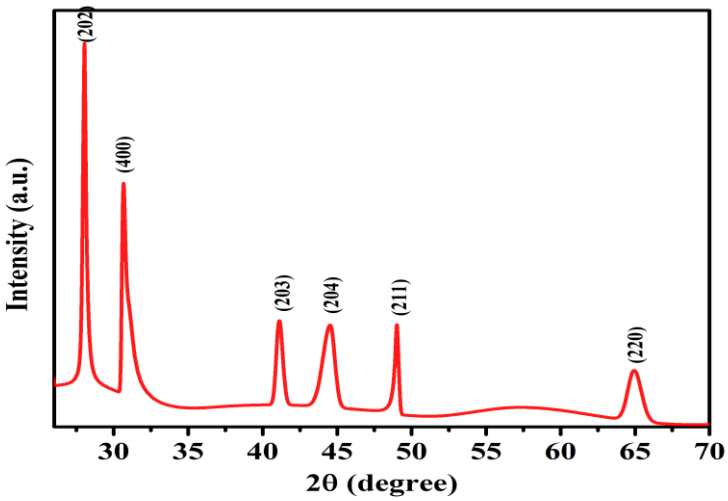

Fig. 3.4: X-Ray diffraction pattern of synthesized nano-powder of BTO

3.4.2 Surface Analysis and EDX

We have studied the surface morphology of the synthesized sample by SEM operated at 20kV and EDX. **Figure 3.5** shows the SEM micrographs of $BaTiO_3$. A careful examination of Figure 3.5 demonstrate that SEM images depict tubular configuration with porous nature of the nanomaterial. Inside the porous tubular structure free space is there and which are generally distributed with grains and termed as pores [19-21]. The centre of the adsorption process is generally performed by these pores. These pores are unconditionally promising for the sensing mechanism of gas. The variation in sensing property of the nano BTO may be observed due to macro porous structure with greater surface area and adsorption when comes in contact with air and CO_2. **Figure 3.5** shows the SEM micrographs of $BaTiO_3$.

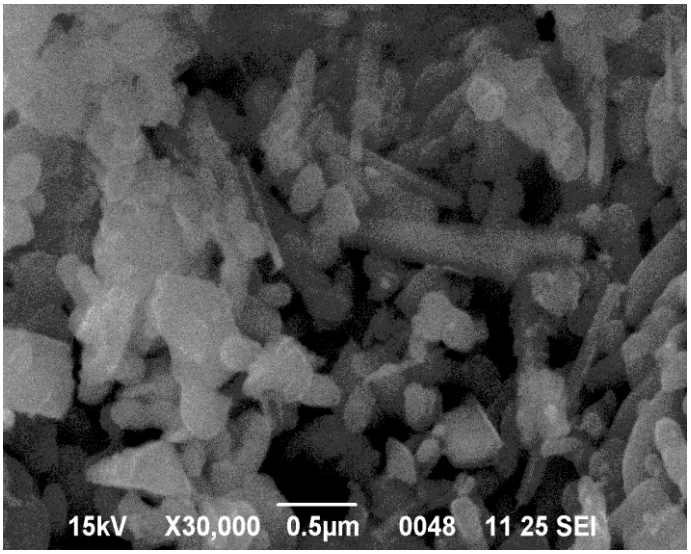

Fig. 3.5: SEM micrographs of $BaTiO_3$

The Elemental Dispersive X-ray (EDX) spectrum has been shown the in following figure. **Figure 3.6** represents the EDX spectrum of synthesized $BaTiO_3$. The EDX spectrum supports the development of barium titanate consisting of Ba 24.07%, Ti 22.78%, O 53.15% in the sample.

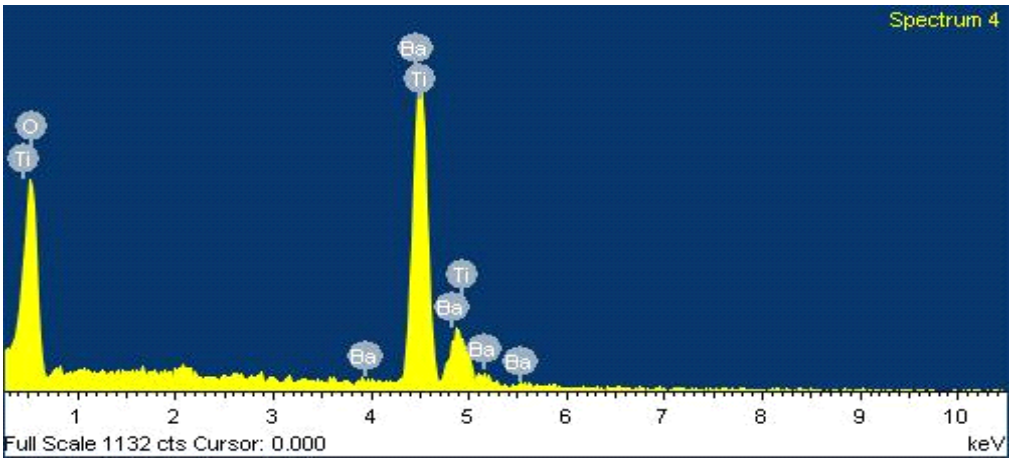

Fig. 3.6: EDX of synthesized $BaTiO_3$

3.4.3 TEM Analysis

TEM analysis was done by TECNAI 200 KV TEM (Fei, Electron Optics), AIIMS Delhi. **Figure 3.7** represents the TEM images of synthesized barium titanate. The sample was furnished by distributing the barium titanate powder in ethanol. Sonication was done for repeatedly many times using ultrasonicator, and a very few drops of floating solution was deposited on grid. The representation at 500 nm scale express the periodic arrangement of particles in a regular form and the image reveals the unique structure of sugarcane stems like formation.

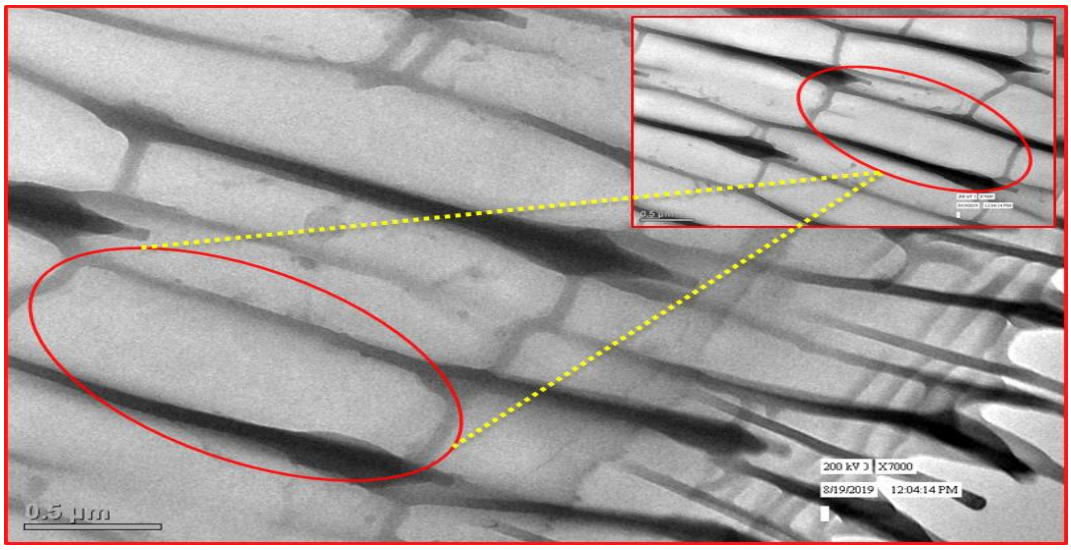

Fig. 3.7: TEM image of $BaTiO_3$

3.4.4 UV-Visible Absorption Spectroscopy

The optical absorbance spectrum of synthesized barium titanate has been shown in **Figure 3.8**. The change in the optical density occurs with the variation in the wavelength and is represented graphically. In addition to this, the obtained data was analysed by the following relationship for calculating the optical band gap energy (E_g):

$$\alpha h\nu = A(h\nu - E_g)^n \text{- - -} (3.1)$$

Where, A is constant. $\boldsymbol{\nu}$ is frequency of transition and the "n" is the value of exponent denoting nature of transition of band (n = 1/2 and n = 3/2 analogous to indirect allowed and forbidden transitions respectively). Optical band gap of synthesized BTO was calculated. The figure shows that it is calculated by extrapolating on energy axis [(hν) versus $(\alpha h\nu)^2$] and the band gap is found as 4.3 eV [22].

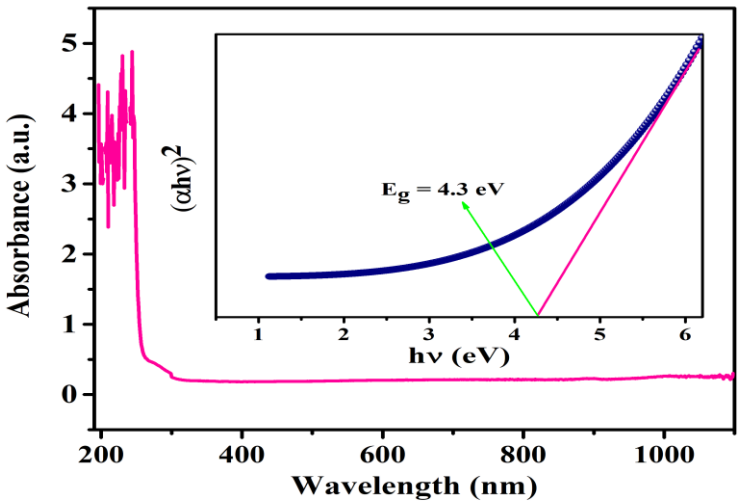

Fig. 3.8: Graphical representation of UV-Vis spectrum of synthesized $BaTiO_3$.

3.4.5 FTIR Analysis

The Fourier transform infrared (FTIR) spectra of the barium titanate was measured at room temperature by the instrument Thermo Nicolet, (Model No. 6700,

USIC, BBAU Lucknow) in the range of wavenumber 4000-500cm^{-1}. The spectrum was recorded by using KBr pellet mixed in 1:15 ratio. Moreover, the spectrum of the sample was acquired in transmittance mode. The pure nano structure of the barium titanate FITR spectra has been shown in the **Figure 3.9**. The bands at 3824.77 and 3422.23cm^{-1}, correspond to the stretching vibrations; moreover, symmetric and asymmetric vibrations of loosely bound water interact with environment through hydrogen bonding and represent stretched vibrations of hydrogen bonded OH groups [23]. The bands at 2920.48 and 2854.41 cm^{-1} represent the adsorption of CH_2 groups [24]. The 1623.41 cm^{-1} band, (i.e. bending mode of H_2O) points out that some H_2O is present [25]. The strong absorption peak at 1453.17 cm^{-1} denotes the asymmetric stretching of impurity, i.e. carbonate ion. The peak at 850cm^{-1} represents the vibrational characteristic of the TiO_2. The peak at 548 cm^{-1} is for the absorption band of $BaTiO_3$ [23].

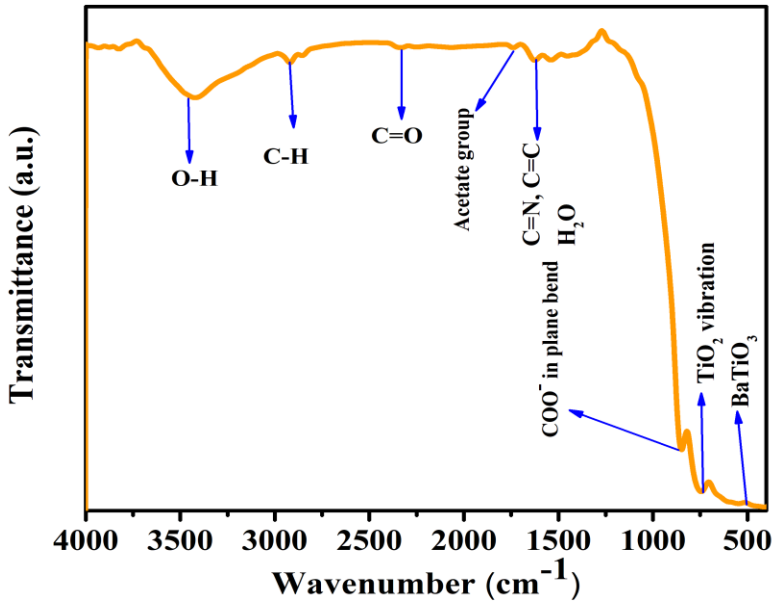

Fig. 3.9: FTIR spectrum of $BaTiO_3$

3.5 Application of Synthesized Barium Titanate

3.5.1 Sensing Behaviour of Barium Titanate Film

In unit cell of barium titanate, there are two cations, i.e., Ba^{2+} and Ti^{4+}. For the B positional cations the coordination number is six, representing octahedral sites and for A cations coordination number is 12. That is the perovskite crystal structure. We verify the CO_2 sensing property of thin film of $BaTiO_3$ by varying concentration of CO_2. Every curve shows the variation of resistance of the film with exposure of CO_2. Initially, the resistance was stabilized at 165 MΩ when film was uncovered to 250 ppm of CO_2 gas. Then the resistance is sharply increases to attain a value of 250 MΩ. The chamber outlet is opened to decrease the resistance, so that it can reach to its initial value around 175 MΩ. This small variation in initial resistance is due to the production of water content by chemical reaction. As much the concentration of gas increases from 250 to 1250 ppm, we have observed the linear variation in sensor response too. The sensor response is also increased in same way as sensitivity shown in **Figure 3.10(c)** and **Figure 3.10(d)**. As CO_2 concentration rises, the amount of gas molecules rises in the chamber and they create dangling bonds on the surface of film so that sensitivity increases. Minimum response time was found 25 s for 250 ppm of CO_2 and recovery time was found as 30 s for 250 ppm of CO_2.

3.5.2 Device Fabrication

To measure the resistance of the sensing element a holder was designed. The sensing element made of thin film of $BaTiO_3$ with a thickness of 1 cm length and ~500 nm thickness was placed. Then it was placed in the middle of the Ag electrodes. The Ag electrodes are square in shape and having a gap in between them is of 0.5 cm with a side length of 0.25 cm. Then a Keithley Electrometer 6514 B and the holder were properly connected together. After that the holder was positioned accurately

inside a closed chamber. With the variations in the CO_2 concentration in the chamber there will be differences in values in resistance of the thin film which is recorded by the electrometer. During the entire experiment, a constant temperature was maintained inside the electrometer. The concentrations of gas inside the chamber were ranged between 250 ppm to 1250 ppm by means of a controlled mass flow meter.

3.5.3 Performance Evaluation of Synthesized $BaTiO_3$ for the Sensing of CO2 Gas

In the beginning of the experiment, the thin film of $BaTiO_3$ was kept for 15 min inside a vacuum chamber to decrease the effect of surface contaminants and made it more stable. Then stabilized resistance as R_a was recorded after stabilization of thin film. After that, the differences in the resistance of the thin film of $BaTiO_3$ exposed to different CO_2 concentrations were observed. The differences in the resistance of the thin film of $BaTiO_3$ with the time before and after exposure to different ppm of CO_2 gas in the closed chamber at room temperature has been shown in **Figure 3.10(a).**

When the thin film was exposed to 250 ppm of CO_2 gas, the first sensing curve with first peak was recorded, which displays a constant variation in resistance and showed less sensing response. Then the thin film was exposed to higher concentration of CO_2 gas (500 ppm) and peak of the second sensing curve showed higher sensing response than the earlier one. Again the film was exposed to highest concentration of CO_2 (1250 ppm) in the chamber and maximum (1.46) sensing response was recorded. But the response and recovery time increases with increase in exposure to 1250 ppm of CO_2. Similarly, there was an observation of decrease in the sensing response while increasing the concentration of CO_2 inside the chamber. This

may be due to fill up of the entire free lattice site on the external surface of the thin film.

The maximum sensor response of $BaTiO_3$ based CO_2 sensor was observed at 1250 ppm shown in **Figure 3.10(c)**. The response time was measured and found as 25 s and recovery time was measured and found as 30 s as shown in **Figure 3.10(b)**. When the film comes in contact with the CO_2 gas, the resistance of $BaTiO_3$ film increases from primary value then after some time it becomes constant. When the chamber outlet is opened, the resistance again approaches to reach its initial value. When CO_2 gas is present in the gas chamber, sensor response changes to R_g from initial value of R_a in accordance with changing gas concentration as shown in **Figure 3.10(a)**. The CO_2 gas sensor of $BaTiO_3$ film gives maximum sensing response 1.46 for CO_2 concentration of 1250 ppm.

Figure 3.10(c) shows the sensor response of the sensor was increasing on increasing the gas concentration, the highest sensor response (1.46) of the sensor has been found at 1250 ppm. **Figure 3.10(d)** shows that the sensitivity of the sensor was increasing on increasing the gas concentration, the highest sensor response (58 MΩ/sec) of the sensor was found at 1250 ppm.

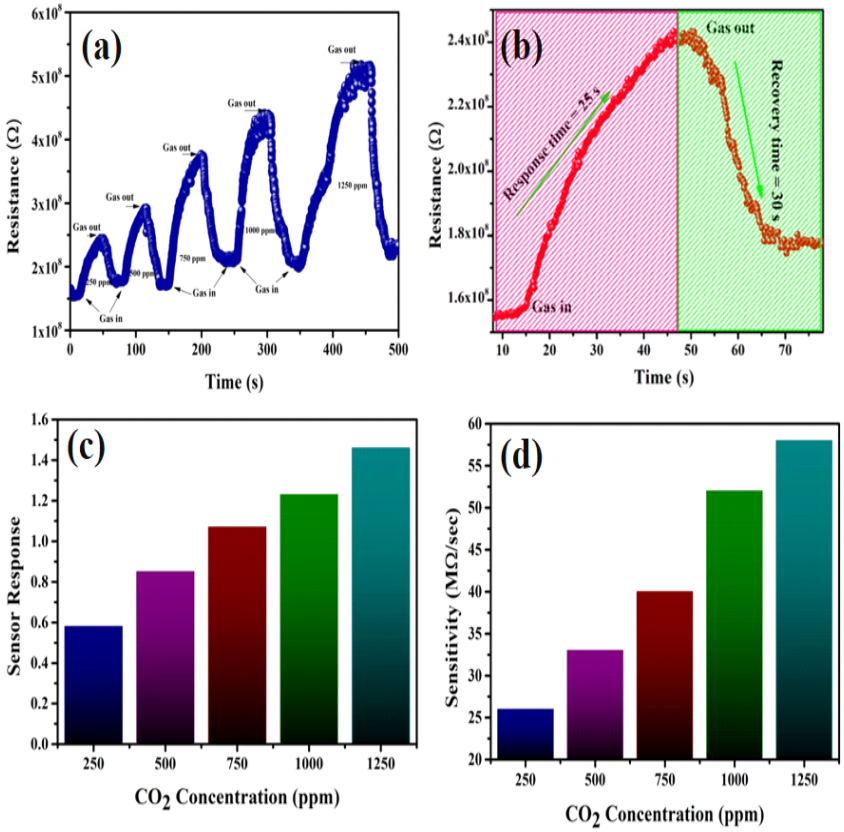

Fig. 3.10(a), 3.10(b), 3.10(c), 3.10(d): Representation of difference in the resistance of the thin film of $BaTiO_3$ at different CO_2 concentrations; Response-Recovery time curve Sensor; Sensor response vs. CO_2 Concentration & Sensitivity vs. CO_2 concentration respectively.

References:

1. K. Abe, T. Tanaka, S. Miura, K. Okazaki, Study on Langev in type $BaTiO_3$ ceramic vibrator, Bulletin of Institute for Chemical Research, Kyoto University, 31 (1953) 295–304.
2. N. Verma, S. Singh, B.C. Yadav, Experimental investigations on barium titanate nanocomposite thin films as an optoelectronic humidity sensor, J. of Experimental Nanosci. 1 (2012) 1-9.
3. T. Takenaka, Piezoelectric properties of some lead-free ferroelectric ceramics, Ferroelectrics, 230 (1999) 87-98.
4. W. Wang, F. Liu, C.M. Lau, L. Wang, G. Yang, D. Zheng, Z. Li, Field-effect BaTiO3Si solar cells, Applied Physics Letters 104 123901 (2014).
5. Y. Okamoto, Y. Suzuki, J. of Physical Chemistry, Mesoporous $BaTiO_3/TiO_2$ Double Layer for Electron Transport in Perovskite Solar Cells, 120 (2016) 139995-14000.
6. T. Tanaka, Barium titanate ceramic and their application, Bulletin of Institute for Chemical Research, Kyoto University, 32(2) (1954) 43-53.
7. Y.K. Mishra, G. Modi, V. Cretu, V. Postica, O. Lupan, T. Reimer, I. Pawlowicz, V. Hrkac, W. Benecke, L. Kienle, R. Adelung, the Direct growth of freestanding ZnO Tetrapod Networks for multifunctional Applications in Photocatalysis, UV- Photodetection and gas sensor, Appl. Mater. Interfaces, 7(26) (2015) 14303-14316.
8. V.R. Chinchamalatpure, S.A. Ghosh, G.N. Chaudhari, Synthesis and Electrical Characterization of $BaTiO_3$ thin films on Si (100), Mat. Sci. and Applications (2010) 187-190.

9. B.D. Stojanovi, A.Z. Simoes, C.O. Paiva-Santos , C. Jovaleki, V.V. Miti, J.A. Varel, Mechanochemical synthesis of barium titanate, Journal of the European Ceramic Society 25 (2005) 1985–1989.

10. Ishihara, T., Kometani, K., Nishi, Y., & Takita, Y. Improved sensitivity of CuO $BaTiO_3$ capacitive-type CO_2 sensor by additives. Sensors and Actuators B: chemical, 28(1) (1995) 49-54.

11. Lee, M. S., & Meyer, J. U. A new process for fabricating CO_2-sensing layers based on $BaTiO_3$ and additives. Sensors and Actuators B: Chemical, 68(1-3) (2000) 293-299.

12. Kareiva, S. Tautkus, R. Papalaviciute, Sol-gel synthesis and characterization of barium titanate powders, J. of Mat. Sci. 34 (1999) 4853-4857.

13. B.R. Li, X.H. Wang, L.T. Li, Synthesis and sintering behavior of BaTiO3 prepared by different chemical methods, Mater. Chem. Phys. 78 (2002) 292-298.

14. C.J. Brinker, G.W. Scherer, Sol-gel Science, The Physics and Chemistry of Sol-gel Processing, Academic Press, Inc., United States of America (1990).

15. W.L. Zhong, Y.G. Wang, P.L. Zhang, B.D. Qu, the Phenomenological study of the size effect on the phase transitions in ferroelectric particles, Phys. Rev. B 50 (1994) 698-703.

16. C.J. Xiao, Z.H. Chi, W.W. Zhang, F.Y. Li. S.M. Feng, C.Q. Jin, X.H. Wang, X.Y. Deng, L.T. Li., The phase transitions and ferroelectric behavior of dense nano crystalline BaTiO3 ceramics fabricated by pressure

assisted sintering, J. of Physics and Chemistry of Solids, 68 (2007) 311-314.

17. M.H. Frey, D.A. Payne, Grain-size effect on the structure and phase transformations for barium titanate, Phys. Rev. B 54 (1996) 3158-3168.

18. Ishihara, T., Kometani, K., Nishi, Y., & Takita, Y. Improved sensitivity of CuO $BaTiO_3$ capacitive-type CO_2 sensor by additives. Sensors and Actuators B: chemical, 28(1) (1995) 49-54.

19. Z.G. Ye, Relaxor ferroelectric complex pervoskites: structure, properties and phase transitions, Key Eng. Material. 155-156 (1998) 81-122.

20. H. Hayashi, T. Nakamura, T. Ebina, In situ Raman spectroscopy of BaTiO3 particles for tetragonal- cubic transformation, J of Phys. and Chem. of Solids 74 (2013) 957962.

21. Michael Veith, Sanjay Mathur, Nicolas Lecere, Volker Huch and Timo Decker, Solgel synthesis of nanoscaled BaTiO3, BaZrO3 and BaTi0.5Zr0.5O3 Oxides via single- source alkoxide precursor and Semi-Alkoxide Route Routes, J. of Sol-Gel Sci. and Tech. 15 (2000) 145-158.

22. D. Lakshmi, V. Meena Priya, J. Shanthi, International journal of information technology & computer sciences study of barium titanate thin films by spin coating technique, 2(1) (2014) 301-303.

23. Dongsheng, F. U., Sue, H. A. O., Jialong, L. I., & Qiang, L. Effects of the penetration temperature on structure and electrical conductivity of samarium modified BaTiO3 powders. Journal of Rare Earths, 29(2) (2011) 164-167.

24. Darwish, A. G. A., Badr, Y., El Shaarawy, M., Shash, N. M. H., & Battisha, I. K. Influence of the Nd3+ ions content on the FTIR and the

visible up-conversion luminescence properties of nano-structure BaTiO3, prepared by sol–gel technique. Journal of alloys and compounds, 489(2) (2010) 451-455.

25. Yang, C. C., Gung, Y. J., Shih, C. C., Hung, W. C., & Wu, K. H. Synthesis, infrared and microwave absorbing properties of (BaFe12O19+ BaTiO3)/polyaniline composite. Journal of Magnetism and Magnetic Materials, 323(7) (2011) 933-938.

CHAPTER 4

CONCLUSIONS AND SCOPE FOR THE FURTHER RESEARCH

This chapter presents all the significant results and discussion of whole research work carried out. Some accompanying key conclusions along with the scope for future researches are given as underneath:

4.1 Conclusions

a) We have done the synthesis of barium titanate successfully using improved sol-gel route.

b) The morphology was observed by FESEM analysis.

c) The crystalline characteristic, formation of phase and minimum crystallite size (9.18 nm) of the barium titanate was confirmed by XRD analysis.

d) The TEM image showed the unique internal structure.

e) The optical band-gap was found to be as 4.3 eV by UV-Vis spectrometer.

f) Further the barium titanate film was fabricated by spin coating method and used for CO_2 sensing application.

g) The maximum sensitivity of the film was found as 58 MΩ/sec at 1250 ppm gas concentration.

h) The sensor response and recovery times were 25s and 30 s respectively.

4.2 Future Scopes

Research is the continuous process which never ends. Although best efforts have been put by the author in the present study, still there is a wide scope o for further research and improvement in present work. Future research works that would be productive in further understanding the role of nano-oxides for low-temperature applications are desirable. These include incorporation of the recovery aspects

achieved by the incorporation of catalyst onto the surface of a nano-oxide being used to detect a reducing gas.

a) In the present work, perovskite structure of barium titanate was optimized to improve the sensing parameters, while there is scope for integration of modifiers like of similar radius or some nano-composite or CNT's for reducing the response and recovery times of CO_2 sensor.

b) We can dope the barium titanate nanomaterial to enhance sensitivity and decrease response and recovery time.

c) An effort may also be made for synthesis of perovskite using various methods and their different sensing applications for comparative study.

d) These results can be compared and the best one can be used for commercialization.

e) The magnetic and dielectric behaviour of perovskite is an interesting area. So attention may be a focus on the twin character of perovskite.

f) The effects of higher annealing temperature on the thin films, substrate, doping, substitution, magnetic field, along with the stability of material may be studied in future.

g) Detailed analysis of the evolution of the surface reactions with respect to temperature needs to be carried out, in order to exactly understand the reaction products from the surface interaction.

h) The application based on surface interaction can be done because of its particle structure, so by testing its toxicity it can be used in biological field also.

i) Growth simulations and reconstructions of the different surface species under different synthesis conditions would give rise to even more specific

engineering of nanomaterial than what is currently known to the world of research within nanotechnology. Spectroscopic evaluation of the sensing mechanism has been important in future research.

j) Theoretical modelling related to the sensing mechanism can be undertaken for further research.

List of publications

Kar, B., Roy, D., Goutam, S.P. and Yadav, A.K., 2019. Perovskite Structured Nanomaterials: An Advanced Key for Global Development of Nanotechnology. *Sensor Letters*, *17*(10), pp.787-791.

List of communicated manuscript

B. Kar et al.; Synthesis, characterization of barium titanate ($BaTiO_3$) & its applications as CO_2 sensor (communicated)

List of conference attended

Kar, B., Roy, D., Goutam, S.P. and Yadav, A.K., 2019. Perovskite structured nanomaterials: An advanced key for global development of nanotechnology. Paper presented in TEQIP-III Sponsored National Conference on Recent Advances in Chemical Sciences (NCRACS-2019) organized by the Applied Science Department, M. M. M. University of Technology, Gorakhpur, March 29-30, 2019.